Table 1. Association of rs2275294 in *ZNF512B* with ALS

	No. of subjects		Risk allele frequency			Odds ratio (95% CI)
	Case	Control	Case	Control	*P*-value	
Discovery series	454	958	0.491	0.422	6.3×10^{-4}	1.32 (1.13–1.55)
Sample set 1	249	1030	0.512	0.434	1.8×10^{-3}	1.37 (1.12–1.66)
Sample set 2	602	2256	0.481	0.416	5.6×10^{-5}	1.30 (1.14–1.48)
Combined	1305	4244				
Meta-analysis[a]					9.3×10^{-10}	1.32 (1.21–1.44)
Joint analysis					6.7×10^{-10}	1.32 (1.21–1.44)

[a]By the Mantel–Haenszel method.

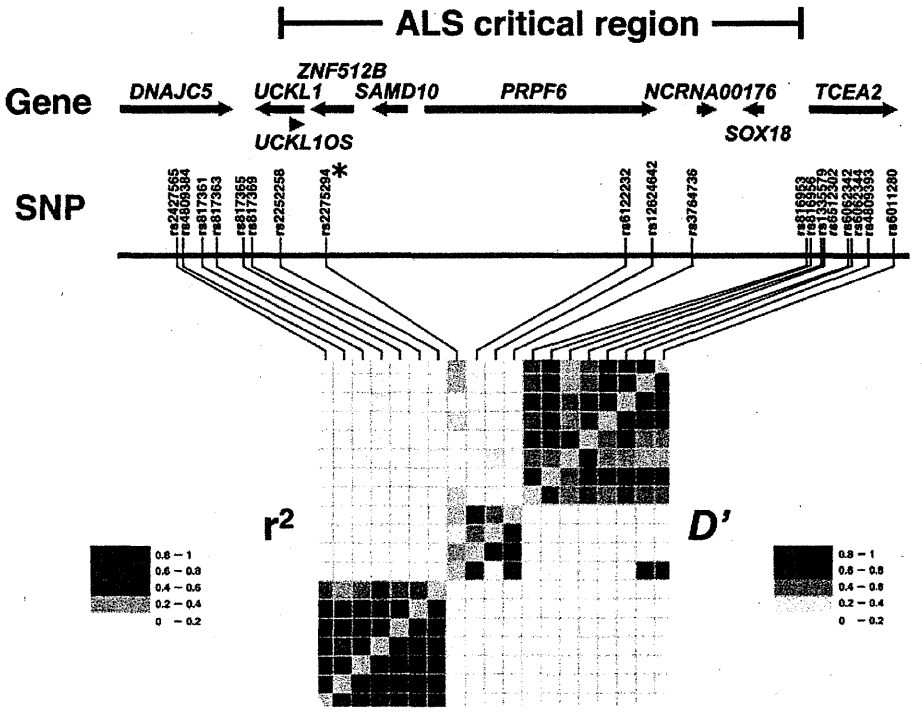

Figure 1. Genomic structure and linkage disequilibrium (LD) map in the ALS critical region. Top, an SNP map of a 111 kb genomic region containing *ZNF512B*. The orientation of each gene is indicated by a green arrow. An asterisk shows the landmark SNP. Bottom, an LD map as measured by D' (lower right triangle) and r^2 (upper left triangle).

examined and no significant differences in age and gender distribution were found among rs2275294 genotyped. The associations with rs2275294 were significant in two sample sets ($P = 4.1 \times 10^{-3}$ and 1.4×10^{-4}), even after adjusting for age and gender in a logistic regression analysis.

Genome analysis of the ALS critical region containing rs2275294

We constructed a linkage disequilibrium (LD) map around rs2275294 on the basis of the genotyping data for Japanese subjects used in HapMap (HapMap JPT). Because rs2275294 was unmapped in the HapMap data, we genotyped the SNP for the HapMap JPT samples and integrated the data with the HapMap JPT data. We found that rs2275294 was in strong LD with the two SNPs rs6122232 and rs3764736 ($D' > 0.85$). Subsequently, the critical region could be confined to a 111 kb interval flanked by rs2252258 and rs816953 on chromosome 20q13.33 (Fig. 1). This region included four genes (*ZNF512B, SAMD10, PRPF6* and *SOX18*) and a part of *UCKL1*, as well as two non-protein-coding RNAs (*UCKL1OS* and *NCRNA00176*). In order to identify a more significantly associated SNP, we searched for SNPs in each gene by re-sequencing genomic DNA of 48 ALS subjects. A total of 24 SNPs were identified and their level of association was examined using 455 cases and 452 controls, but rs2275294 remained the most significantly associated (Supplementary Material, Table S3).

Functional analysis of rs2275294

To gain insight into the biological significance of rs2275294, luciferase reporter plasmids corresponding to a genomic

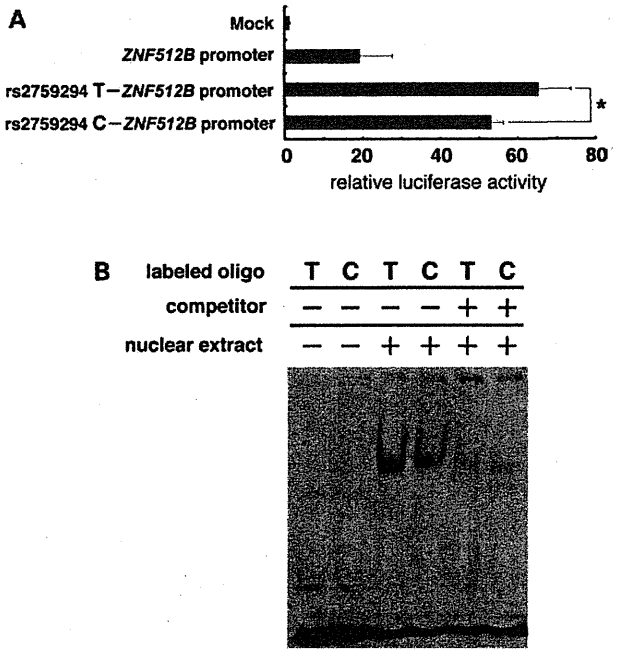

Figure 2. Functional analysis for rs2275294 in *ZNF512B*. (**A**) Difference in the enhancer activity of genomic DNA segments containing rs2275294. Luciferase assay in SK_N_Be(2)C cells. Enhancer activity was lower in the ALS-susceptibility allele (C allele). *ZNF512B* promoter:native promoter (nts −820 to −74) of *ZNF512B*. Data represent the mean ± SEM ($n = 6$). *$P < 0.01$ (Student's t-test). (**B**) Difference in binding of nuclear proteins to a cis-element containing rs2275294. An EMSA using nuclear extracts from SK_N_AS cells. The specific band was weaker in the ALS-susceptibility allele (C allele).

DNA fragment containing rs2275294 were constructed and a luciferase assay using the human neuroblastoma cell line SK_N_Be(2)C was performed. Constructs containing the ALS-susceptibility allele (C allele) of rs2275294 showed lower enhancer activity than those containing the non-susceptibility allele, indicating that the SNP affects the *ZNF512B* transcription level (Fig. 2A). We then examined the allelic difference in the binding of genomic DNA containing rs2275294 to nuclear proteins by the electrophoretic mobility shift assay (EMSA). The DNA–protein complex from the C allele showed weaker binding (Fig. 2B). Thus, it is feasible that the presence of the susceptibility allele leads to lower *ZNF512B* levels as a consequence of decreased enhancer activity.

ZNF512B is a positive regulator in the TGF-β signaling pathway

Proteomics analysis has suggested that ZNF512B functions as a regulator of the TGF-β signaling pathway (54). We examined the effect of ZNF512B on TGF-β signaling using the TGF-β-dependent SMAD2/3-specific luciferase assay (55) in a HepG2 cell (data not shown). SMAD2/3-mediated reporter activity after TGF-β stimulation was enhanced by ZNF512B over-expression. The TGF-β-dependent reporter activity was activated by ZNF512B over-expression in a neuroblastoma

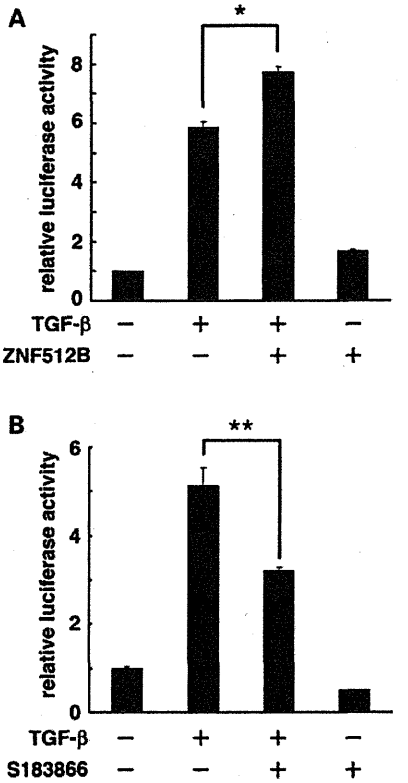

Figure 3. ZNF512B is a positive regulator of the TGF-β signal. (**A**) Luciferase assay using SBE4-luciferase. ZNF512B trans-activated the TGF-β-induced SMAD transcriptional activity in the SK_N_AS cell line (*$P < 0.0005$). (**B**) S183866, a *ZNF512B*-targeting siRNA oligonucleotide repressed the TGF-β-dependent SBE4-luciferase activity (**$P < 0.005$).

cell line SK_N_AS (Fig. 3A) and a glioblastoma cell line U87MG (Supplementary Material, Fig. S4). Next, we knocked down expression of the endogenous *ZNF512B* in SK_N_AS by using the short-interfering RNA (siRNA) technique. Real time polymerase chain reaction (PCR) showed that *ZNF512B* siRNA significantly reduced *ZNF512B* transcription, and TGF-β-dependent reporter activity was repressed by the siRNA (Fig. 3B).

ZNF512B expression in the spinal cord of ALS

The localization of ZNF512B in the spinal cord of ALS patients was investigated by immuno-histochemical studies. The immuno-reactivity for an anti-ZNF512B polyclonal antibody was intense in motor neuron cells in the anterior horn of the spinal cords of ALS patients, while it was barely detectable in those of controls (Fig. 4A–D). Glial cells in the anterior horn did not show ZNF512B immuno-reactivity.

DISCUSSION

By a large-scale case–control association study using gene-based SNPs and enrolling a total of more than 5500 subjects, we identified *ZNF512B* at chromosome 20q13.33 as a new susceptibility gene for ALS. rs2275294 in *ZNF512B* had

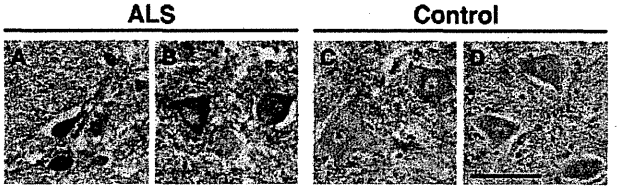

Figure 4. Immuno-histochemical localization of ZNF512B in the spinal cord of ALS patients (**A** and **B**) and controls (**C** and **D**). The ZNF512B immuno-reactivity was intense in motor neuron cells in the anterior horn of ALS patients, while it was hardly detectable in those of controls. Glial cells in the anterior horn did not show ZNF512B immuno-reactivity. Scale bar, 100 μm.

significant association that satisfied a genome-wide significance level ($P = 9.3 \times 10^{-10}$). rs2275294 affected *ZNF512B* transcription *in vitro*, and the ALS-susceptibility allele (C allele) showed lower enhancer activity for the *ZNF512B* promoter. Therefore, *ZNF512B* is presumably lower in those who have the susceptibility allele than in those who have the non-susceptibility allele. *ZNF512B* over-expression enhanced TGF-β signaling, while its knockdown decreased the signal. Our findings suggest that ZNF512B is an important positive regulator of TGF-β and that lowered ZNF512B expression is implicated in the pathogenesis of ALS susceptibility via decreased TGF-β signal.

In this study, we screened the genic regions using >52 000 gene-based SNPs from the JSNP database. The number of SNPs and their coverage are not sufficient to screen the entire genome. Our study must have many false negatives. Current commercial GWAS platforms are considered superior to ours in terms of the study power and the coverage of SNPs in the human genome. In contrast, the false-positive association of rs2275294 is unlikely. The inflation factor was low and principal component analysis showed no evidence of population stratification. We validated the association in independent Japanese panels. The statistical significance of the association for the combined *P*-values by two different methods fulfilled criteria of the genome-wide significance level. The results of the two analyses were very similar, which further shows that a hidden confounder in our population is unlikely. In addition, there was no difference in the population structures among the case–control sets by Wright's F statistics (53) throughout the study. The MAF of rs2275294 in 744 Japanese samples deposited in dbSNP is similar to that of our controls (0.414).

In spite of its very significant association in our study, rs2275294 in *ZNF512B* has not been found in the previous GWASs. Several explanations can be considered. The main reason is that rs2275294 was not included in the platforms of the previous GWASs. Only 15 SNPs in Illumina 610K SNP Array were mapped to the 111 kb genomic region (1 SNP/7.4 kb) corresponding to the ALS critical region we determined. Also, only 10 SNPs in Affymetrix SNP Array 6.0 were mapped to the genomic region (1 SNP/11.1 kb). In addition, rs2275294 is not even mapped in the HapMap JPT database, nor included in the CEU and YRI HapMap data sets. In the Illumina and Affymetrix SNP arrays, the numbers of SNPs in the *ZNF512B* locus are only two and one, respectively. Their coverages of *ZNF512B*-SNPs in the ALS critical region were very low, 2/15 (13%) and 1/10 (10%), respectively. The low coverage of the region might have led to the false-negative association in the previous GWASs. No SNP was in strong LD ($r^2 > 0.8$) with rs2275294 in CHB-JPT, CEU and YRI in the 1000 Genomes data (Supplementary Material, Table S4). Hence, we speculate that rs2275294 has been identified by virtue of our platform. Still another explanation is the ethnic difference of ALS susceptibility.

A number of GWASs in ALS have been performed recently. They report the identification of five candidate genes and two candidate loci (30–35). Among them, only five gene loci (*DPP6*, *ITPR2*, *FLJ10986*, *KIFAP3* and *UNC13A*) were included in our platform. We checked 16 SNPs in *DPP6*, 23 in *ITPR2*, 2 in *FLJ10986*, 9 in *KIFAP3* and 4 in *UNC13A*; however, their associations were not replicated in our study (Supplementary Material, Table S5). The small number of samples and the low coverage of SNPs in our platform may have resulted in false-negative association. Ethnic differences may be another reason for no replication. The 9p21.2 SNP that has been reported in the previous study (42) was not included in the present study. The tested SNPs for previous associations were negative, but no evidence can be provided for the chromosome 9p21.2 locus. Because the powers of Japanese and Chinese were only 0.37 and 0.11, respectively (42), the negative association may be due to a lack of power in the study. More extensive association studies using larger panels of Japanese samples will be required to conclude the associations between previous candidate genes and ALS.

ZNF512B was originally identified as a *KIAA1196* in the course of the Kazusa Human cDNA project (56). The *ZNF512B* cDNA is 5919 bp long and encodes an 893 amino-acid protein that is ubiquitously expressed in various tissues, including the brain and spinal cord (56). Our immunohistochemical studies confirmed its localization in the spinal cord. The ZNF512B protein showed no significant homology with any proteins in the public database. It contains six C2H2-type zinc finger domains and is predicted to act as a transcription factor. The ALS-susceptibility SNP rs2275294 was localized to intron 12 of *ZNF512B*. We have demonstrated that the genomic region containing rs2275294 can act as an enhancer of the *ZNF512B* promoter and that the susceptibility allele of rs2275294 had reduced transcriptional activity, which was likely due to its decreased binding capacity to trans-factors. Further studies for the upstream factors of *ZNF512B* are necessary to clarify the molecular pathogenesis of ALS related to *ZNF512B*.

We showed that ZNF512B is a positive regulator of the canonical TGF-β signaling pathway through SMAD2/3. TGF-β signal is essential for the survival of neurons (44–46). Upregulation of PAI-1 by SMAD3-dependent induction in astrocytes mediates the neuroprotective activity of TGF-β against NMDA receptor-mediated excitotoxicity (57). TGF-β signal has been implicated in the pathogenesis of ALS. Plasma TGF-β1 level is significantly increased in ALS patients compared with healthy controls, and there is a significant positive correlation between TGF-β1 concentration in ALS patients and duration of their disease (58). A microarray analysis showed a 4.8-fold increased expression of *SMAD4* in sALS compared with neurologically normal controls (59).

Also, phosphorylated SMAD2/3 immuno-reactivity is increased in the remaining spinal motor neurons and glial cells in sporadic and familial ALSs, as well as in *Sod1* transgenic mice (60). These findings suggest that the TGF-β signal is increased in ALS.

Several studies have shown an association between duration of ALS and TGF-β levels. Houi *et al.* (58) found a positive correlation between the plasma concentration of TGF-β1 in ALS patients and the duration of disease. Another group reported that TGF-β1 concentrations in serum and cerebrospinal fluid did not differ between ALS patients and controls, but were higher in ALS patients with a terminal clinical status than in controls (61). These data suggest that TGF-β is increased in the motor neuron cells of ALS patients during the disease process. As ZNF512B is a critical enhancer of TGF-β signaling, its genetic association may be related to the progression of the disease rather than its onset.

We have demonstrated the localization of ZNF512B in the spinal cord of ALS patients, and that ZNF512B expression in the motor neurons of ALS patients was significantly increased compared with that of controls (Fig. 4). It is biologically plausible that ZNF512B is a positive regulator (co-activator) of neuroprotective TGF-β signaling (Fig. 3) and may act as a protector against ALS. Taken together with the results of luciferase assay and EMSA that showed allelic differences in *ZNF512B* expression level (Fig. 2), a patient harboring the susceptibility allele would have decreased *ZNF512B* expression level compared with a patient harboring non-susceptibility alleles. The decreased *ZNF512B* enhancer activity by the susceptibility allele leads to insufficient increase in ZNF512B, which leads to insufficient increase in the TGF-β signal that results in decreased potential for survival and/or recovery of motor neurons. The discovery of this ALS-susceptibility gene and its pathway should shed light on ALS pathogenesis and facilitate development of targeted therapies.

MATERIALS AND METHODS

Subjects

A total of 1305 ALS patients diagnosed as having probable, probable and laboratory-supported, or definite ALS according to the El Escorial revised criteria (62) were included in the study. All subjects were unrelated Japanese individuals. We obtained a total of 703 DNA samples from the Biobank Japan project (63). All patients were screened for mutations in *SOD1*, *TARDBP* and *ANG* and none was detected. The mean age of cases was 60.8 years (range: 28–82 years), and 66.1% were male. 74.4% had a spinal onset, 19.6% a bulbar one and 6% a multiple and the others. We obtained a total of 602 DNA samples from the Japanese Consortium for Amyotrophic Lateral Sclerosis Research (JaCALS), Jichi Medical University and The University of Tokyo. The mean age was 61.5 years (range: 27–89 years), and 62.0% were male. 70.4% of the patients had a spinal onset and the remaining had a bulbar one. We recruited 4244 controls through several medical institutes in Japan. Their mean age was 66.8 years (range: 18–98 years), and 48.0% were male. All controls had negative medical and family histories for neurodegenerative disorders. Written informed consent was obtained from all the subjects. The ethical committees at the participating institutions approved this project.

SNP genotyping

Using standard protocols, genomic DNA was extracted from the peripheral blood leukocytes. SNPs were genotyped using the multiplex PCR-based invader assay (Third Wave Technologies) as described previously (64). A total of 52 608 gene-based SNPs were selected from the JSNP database on the basis of the haplotype block structure reported previously (43,65). We calculated the total number of independent SNPs in this study to be 43 052 (the SNPs in LD: $r^2 > 0.80$ were considered as one SNP). We checked the cryptic relatedness for each pair of samples by identity-by-state by estimating the average number of shared alleles between two individuals (V_I) using 48 884 autosomal SNPs. Six individuals in controls were related ($V_I > 1.65$). They were excluded from the analysis. A stepwise screening method was adopted to increase the statistical power (66). In stage 1, 92 ALS and 233 control subjects were analyzed. We applied the SNP quality control filters of call rate of ≥ 0.95 in both cases and controls and *P*-value of Hardy–Weinberg equilibrium (HWE) test of $\geq 1.0 \times 10^{-2}$ in controls. A total of 48 939 SNPs on autosomal chromosomes passed the quality control filters and were analyzed for the association. The data of this study are available at the JSNP database (http://snp.ims.u-tokyo.ac.jp/). Among the SNPs analyzed in stage 1, 893 SNPs showing the smallest *P*-values (0.01 or smaller) were selected for stage 2. Three models (i.e. allelic, dominant and recessive) were tested for the association. Since these three models are not independent, 893 SNPs were isolated. In stage 2, we genotyped an additional 1087 subjects consisting of 362 ALS cases and 725 controls. Stage 1 and stage 2 were defined as the discovery series of this research and the following sample sets were defined as sample set 1 and sample set 2.

SNP discovery

Appropriate genome sequences were extracted from the UCSC Genome Bioinformatics website. The critical region contained five genes (*ZNF512B, SAMD10, PRPF6, SOX18* and part of *UCKL1*) and two non-protein-coding RNAs (*UCKL1OS* and *NCRNA00176*). We defined the exon–intron boundaries of each gene and designed PCR primer sets for the critical region except for repetitive sequence regions. Each PCR was performed with 5 ng of mixed genomic DNA derived from three ALS subjects; 16 mixed samples were amplified in the GeneAmp PCR system 9700 (PE Applied Biosystems) under the following conditions: initial denaturation at 95°C for 2 min, followed by 35 cycles of denaturation at 96°C for 30 s, annealing at 60–65°C for 30 s, extension at 72°C for 2 min and post-extension at 72°C for 7 min. PCR products served as templates for direct sequencing by the fluorescent dye-terminator cycle sequencing method.

Statistical analysis

For general statistical analyses, we used R statistical environment version 2.6.1 and programs created by our group. The Chi-square test or Fisher's exact test was applied to a two-by-two contingency table in three genetic models: an allele frequency model, a dominant-effect model and a recessive-effect model. Principal component analysis was performed using the smartpca program (52). We calculated the association in case–control status of stage 1 by using a twstats of EIGENSOFT (52). The top six principal components were associated with case–control status. Genotype data from the HapMap project were used (67) to estimate the population structure. The significance of stratification was determined using the Wright method (53). The Mantel–Haenszel method was used for meta-analysis. An automated laboratory system and bar-coding were employed to reduce clerical errors. The accuracy of our system has been guaranteed in data of the HapMap project (67). We checked HWE and personally retyped some SNPs from genome screening in duplicated samples. We also obtained age- and gender-adjusted odds ratios by logistic regression analysis by program R. Haploview 4.1 was used to infer the LD structure of the ALS critical region. An LD pattern was created based on the JPT HapMap data. Luciferase assay data were analyzed by Student's *t*-test.

Luciferase assay

We cloned DNA fragments containing rs2275294, nucleotides (nts) 190–208 of intron 12 of *ZNF512B*. The fragments for both alleles as three tandem copies were inserted into pGL3-Basic vector (Promega) upstream of its luciferase gene in 5′−>3′ orientation together with the *ZNF512B* core promoter of nts −820 to −74 of its 5′ flanking region. We transfected SK_N_Be(2)C cells with 400 ng of each reporter construct using FuGene 6 transfection reagent (Roche) together with 8 ng of pRL-TK vector (Promega) as a control. After 24 h, the cells were lysed in a passive lysis buffer and luciferase activities were measured using Dual-Luciferase Reporter Assay System (Toyo Ink). The entire coding sequence of ZNF512B was cloned into pcDNA3.1, which had a Myc-tag sequence. We also co-transfected with SBE4 (four copies of Smad Binding Element) luciferase reporter vector (55)/Myc-tagged ZNF512B or SBE_4-luciferase reporter vector/Myc-tagged pcDNA3.1, and pRL-TK vector using Trans-IT LT reagent (TAKARA Bio). After 24 h, we treated the cells with 10 ng/ml of TGF-β for 24 h. The cells were lysed in a passive lysis buffer and luciferase activities were measured using Dual-Luciferase Reporter Assay System (Toyo Ink).

Electrophoretic mobility shift assay

A nuclear extract from SK_N_AS cells was prepared as previously described (68) and incubated with oligonucleotides (nts 184–203 of intron 12 of *ZNF512B*) that were labeled with digoxigenin-11-ddUTP using the Dig Gel Shift Kit (Roche). The reaction was carried out at a room temperature with an additional 1 mg/ml of poly[d(I-C)]. For the competition assay, the nuclear extract was pre-incubated with unlabeled oligonucleotides (200-fold molar excess) before adding digoxigenin-labeled oligonucleotide. The protein–DNA complex was separated on a non-denaturing 6% polyacrylamide gel in 0.25× Tris-borate-EDTA buffer. We transferred the gel to membrane and detected the signal with a chemiluminescent detection system (Roche) according to the manufacturer's instructions.

RNAi experiment

Double-strand stealth RNAi oligonucleotides (ZNF512B-S183866 for ZNF512B and negative universal control medium GC duplex for negative control) were purchased from Invitrogen. The RNAi oligonucleotides were transfected into a cell line using Lipofectamine RNAiMAX reagent according to the manufacturer's instructions (Invitrogen). After 24 h, we also transfected with SBE_4-luciferase reporter vector and pRL-TK vector. We treated the cells with TGF-β (10 ng/ml) for 24 h, collected the cells and measured luciferase activity using the Dual-Luciferase Reporter Assay System (Toyo Ink).

Immuno-histochemistry

Autopsy specimens of lumbar spinal cord were obtained from clinically and histopathologically diagnosed ALS patients (13 males and 9 females, age 41–79 years) and from neurologically normal patients (4 males and 3 females, age 42–76 years). The autopsy times in relation to death for the cases and controls (average ± SD) were 4.0 ± 2.8 h and 4.5 ± 5.2 h, respectively. 6-μm-thick sections were prepared from paraffin-embedded tissues. The sections were microwaved for 20 min in 50 mM citrate buffer (pH 6.0) and then treated with a TNB blocking buffer (PerkinElmer) before incubation with an anti-ZNF512B antibody (Santa Cruz Biotechnology, 1:200). The immuno-reactivity was detected using EnVision+ System-HRP (Dako). The sections were photographed with an optical microscope (BX51, Olympus).

SUPPLEMENTARY MATERIAL

Supplementary Material is available at *HMG* online.

ACKNOWLEDGMENTS

We thank all ALS patients who participated in the study. We also thank all members of Japanese ALS Association and all participating doctors and staff from collaborating institutes. The DNA samples used for this research were provided from the Leading Project for Personalized Medicine in the Ministry of Education, Culture, Sports, Science and Technology, Japan, and from JaCALS. JaCALS members included Drs M. Ito, J. Senda (Nagoya University), H. Takano (Niigata University), A. Kawata, H. Hayashi (Tokyo Metropolitan Neurological Hospital), I. Aiba (Higashi Nagoya National Hospital), A. Taniguchi (Mie University), Y. Izumi (University of Tokushima), M. Sakai, M. Konagaya (Suzuka National Hospital), H. Mizusawa (Tokyo Medical and Dental University), T. Yuasa (Kamagaya General Hospital), T. Fujita (Takumikai

Neurology Clinic), M. Ikeda, K. Okamoto (Gunma University), S. Akimoto, H. Sasaki (Hokkaido University), T. Imai (Miyagi National Hospital) and S. Kuzuhara (National Center Hospital of Neurology and Psychiatry).

Conflict of Interest statement. None declared.

FUNDING

This work was supported by grants from the Leading Project of Ministry of Education, Culture, Sports, Science and Technology Japan; Health and Labour, Sciences Research Grants for Research on Measures for Intractable Diseases and Comprehensive Research on Aging and Health from the Ministry of Health, Labour and Welfare, Japan; and by a Grant-in-Aid for Scientific Research (C) (19500314) from the Ministry of Education, Culture, Sports, Science and Technology Japan (A.I.).

REFERENCES

1. Wijesekera, L.C. and Leigh, P.N. (2009) Amyotrophic lateral sclerosis. *Orphanet J. Rare Dis.*, **4**, 3.
2. Cronin, S., Hardiman, O. and Traynor, B.J. (2007) Ethnic variation in the incidence of ALS: a systematic review. *Neurology*, **68**, 1002–1007.
3. Al-Chalabi, A., Fang, F., Hanby, M.F., Leigh, P.N., Shaw, C.E., Ye, W. and Rijsdijk, F. (2010) An estimate of amyotrophic lateral sclerosis heritability using twin data. *J. Neurol. Neurosurg. Psychiatry*, **81**, 1324–1326.
4. Wroe, R., Wai-Ling Butler, A., Andersen, P.M., Powell, J.F. and Al-Chalabi, A. (2008) ALSOD: the Amyotrophic Lateral Sclerosis Online Database. *Amyotroph. Lateral Scler.*, **9**, 249–250.
5. Yoshida, M., Takahashi, Y., Koike, A., Fukuda, Y., Goto, J. and Tsuji, S. (2010) A mutation database for amyotrophic lateral sclerosis. *Hum. Mutat.*, **31**, 1003–1010.
6. Rosen, D.R., Siddique, T., Patterson, D., Figlewicz, D.A., Sapp, P., Hentati, A., Donaldson, D., Goto, J., O'Regan, J.P., Deng, H.X. *et al.* (1993) Mutations in Cu/Zn superoxide dismutase gene are associated with familial amyotrophic lateral sclerosis. *Nature*, **362**, 59–62.
7. Al-Chalabi, A., Andersen, P.M., Nilsson, P., Chioza, B., Andersson, J.L., Russ, C., Shaw, C.E., Powell, J.F. and Leigh, P.N. (1999) Deletions of the heavy neurofilament subunit tail in amyotrophic lateral sclerosis. *Hum. Mol. Genet.*, **8**, 157–164.
8. Yang, Y., Hentati, A., Deng, H.X., Dabbagh, O., Sasaki, T., Hirano, M., Hung, W.Y., Ouahchi, K., Yan, J., Azim, A.C. *et al.* (2001) The gene encoding alsin, a protein with three guanine-nucleotide exchange factor domains, is mutated in a form of recessive amyotrophic lateral sclerosis. *Nat. Genet.*, **29**, 160–165.
9. Hadano, S., Hand, C.K., Osuga, H., Yanagisawa, Y., Otomo, A., Devon, R.S., Miyamoto, N., Showguchi-Miyata, J., Okada, Y., Singaraja, R. *et al.* (2001) A gene encoding a putative GTPase regulator is mutated in familial amyotrophic lateral sclerosis 2. *Nat. Genet.*, **29**, 166–173.
10. Puls, I., Jonnakuty, C., LaMonte, B.H., Holzbaur, E.L., Tokito, M., Mann, E., Floeter, M.K., Bidus, K., Drayna, D., Oh, S.J. *et al.* (2003) Mutant dynactin in motor neuron disease. *Nat. Genet.*, **33**, 455–456.
11. Nishimura, A.L., Mitne-Neto, M., Silva, H.C., Richieri-Costa, A., Middleton, S., Cascio, D., Kok, F., Oliveira, J.R., Gillingwater, T., Webb, J. *et al.* (2004) A mutation in the vesicle-trafficking protein VAPB causes late-onset spinal muscular atrophy and amyotrophic lateral sclerosis. *Am. J. Hum. Genet.*, **75**, 822–831.
12. Chen, Y.Z., Bennett, C.L., Huynh, H.M., Blair, I.P., Puls, I., Irobi, J., Dierick, I., Abel, A., Kennerson, M.L., Rabin, B.A. *et al.* (2004) DNA/RNA helicase gene mutations in a form of juvenile amyotrophic lateral sclerosis (ALS4). *Am. J. Hum. Genet.*, **74**, 1128–1135.
13. Greenway, M.J., Andersen, P.M., Russ, C., Ennis, S., Cashman, S., Donaghy, C., Patterson, V., Swingler, R., Kieran, D., Prehn, J. *et al.* (2006) ANG mutations segregate with familial and 'sporadic' amyotrophic lateral sclerosis. *Nat. Genet.*, **38**, 411–413.
14. Kabashi, E., Valdmanis, P.N., Dion, P., Spiegelman, D., McConkey, B.J., Vande Velde, C., Bouchard, J.P., Lacomblez, L., Pochigaeva, K., Salachas, F. *et al.* (2008) TARDBP mutations in individuals with sporadic and familial amyotrophic lateral sclerosis. *Nat. Genet.*, **40**, 572–574.
15. Sreedharan, J., Blair, I.P., Tripathi, V.B., Hu, X., Vance, C., Rogelj, B., Ackerley, S., Durnall, J.C., Williams, K.L., Buratti, E. *et al.* (2008) TDP-43 mutations in familial and sporadic amyotrophic lateral sclerosis. *Science*, **319**, 1668–1672.
16. Kwiatkowski, T.J. Jr, Bosco, D.A., Leclerc, A.L., Tamrazian, E., Vanderburg, C.R., Russ, C., Davis, A., Gilchrist, J., Kasarskis, E.J., Munsat, T. *et al.* (2009) Mutations in the FUS/TLS gene on chromosome 16 cause familial amyotrophic lateral sclerosis. *Science*, **323**, 1205–1208.
17. Vance, C., Rogelj, B., Hortobagyi, T., De Vos, K.J., Nishimura, A.L., Sreedharan, J., Hu, X., Smith, B., Ruddy, D., Wright, P. *et al.* (2009) Mutations in FUS, an RNA processing protein, cause familial amyotrophic lateral sclerosis type 6. *Science*, **323**, 1208–1211.
18. Maruyama, H., Morino, H., Ito, H., Izumi, Y., Kato, H., Watanabe, Y., Kinoshita, Y., Kamada, M., Nodera, H., Suzuki, H. *et al.* (2010) Mutations of optineurin in amyotrophic lateral sclerosis. *Nature*, **465**, 223–226.
19. Mitchell, J., Paul, P., Chen, H.J., Morris, A., Payling, M., Falchi, M., Habgood, J., Panoutsou, S., Winkler, S., Tisato, V. *et al.* (2010) Familial amyotrophic lateral sclerosis is associated with a mutation in D-amino acid oxidase. *Proc. Natl Acad. Sci. USA*, **107**, 7556–7561.
20. Beleza-Meireles, A. and Al-Chalabi, A. (2009) Genetic studies of amyotrophic lateral sclerosis: controversies and perspectives. *Amyotroph. Lateral Scler.*, **10**, 1–14.
21. Simpson, C.L. and Al-Chalabi, A. (2006) Amyotrophic lateral sclerosis as a complex genetic disease. *Biochim. Biophys. Acta*, **1762**, 973–985.
22. Schymick, J.C., Talbot, K. and Traynor, B.J. (2007) Genetics of sporadic amyotrophic lateral sclerosis. *Hum. Mol. Genet.*, **16**, R233–R242.
23. Figlewicz, D.A., Krizus, A., Martinoli, M.G., Meininger, V., Dib, M., Rouleau, G.A. and Julien, J.P. (1994) Variants of the heavy neurofilament subunit are associated with the development of amyotrophic lateral sclerosis. *Hum. Mol. Genet.*, **3**, 1757–1761.
24. Hayward, C., Colville, S., Swingler, R.J. and Brock, D.J. (1999) Molecular genetic analysis of the APEX nuclease gene in amyotrophic lateral sclerosis. *Neurology*, **52**, 1899–1901.
25. Greenway, M.J., Alexander, M.D., Ennis, S., Traynor, B.J., Corr, B., Frost, E., Green, A. and Hardiman, O. (2004) A novel candidate region for ALS on chromosome 14q11.2. *Neurology*, **63**, 1936–1938.
26. Skvortsova, V., Shadrina, M., Slominsky, P., Levitsky, G., Kondratieva, E., Zherebtsova, A., Levitskaya, N., Alekhin, A., Serdyuk, A. and Limborska, S. (2004) Analysis of heavy neurofilament subunit gene polymorphism in Russian patients with sporadic motor neuron disease (MND). *Eur. J. Hum. Genet.*, **12**, 241–244.
27. Gros-Louis, F., Andersen, P.M., Dupre, N., Urushitani, M., Dion, P., Souchon, F., D'Amour, M., Camu, W., Meininger, V., Bouchard, J.P. *et al.* (2009) Chromogranin B P413L variant as risk factor and modifier of disease onset for amyotrophic lateral sclerosis. *Proc. Natl Acad. Sci. USA*, **106**, 21777–21782.
28. Blasco, H., Corcia, P., Veyrat-Durebex, C., Coutadeur, C., Fournier, C., Camu, W., Gordon, P., Praline, J., Andres, C.R. and Vourc'h, P. (2010) The P413L chromogranin B variation in French patients with sporadic amyotrophic lateral sclerosis. *Amyotroph. Lateral Scler.*, doi:10.3109/17482968.2011.522587.
29. van Vught, P.W., Veldink, J.H. and van den Berg, L.H. (2010) P413L CHGB is not associated with ALS susceptibility or age at onset in a Dutch population. *Proc. Natl Acad. Sci. USA*, **107**, E77; author reply E78.
30. Schymick, J.C., Scholz, S.W., Fung, H.C., Britton, A., Arepalli, S., Gibbs, J.R., Lombardo, F., Matarin, M., Kasperaviciute, D., Hernandez, D.G. *et al.* (2007) Genome-wide genotyping in amyotrophic lateral sclerosis and neurologically normal controls: first stage analysis and public release of data. *Lancet Neurol.*, **6**, 322–328.
31. Dunckley, T., Huentelman, M.J., Craig, D.W., Pearson, J.V., Szelinger, S., Joshipura, K., Halperin, R.F., Stamper, C., Jensen, K.R., Letizia, D. *et al.* (2007) Whole-genome analysis of sporadic amyotrophic lateral sclerosis. *N. Engl. J. Med.*, **357**, 775–788.
32. van Es, M.A., Van Vught, P.W., Blauw, H.M., Franke, L., Saris, C.G., Andersen, P.M., Van Den Bosch, L., de Jong, S.W., van 't Slot, R., Birve, A. *et al.* (2007) ITPR2 as a susceptibility gene in sporadic amyotrophic lateral sclerosis: a genome-wide association study. *Lancet Neurol.*, **6**, 869–877.

33. van Es, M.A., van Vught, P.W., Blauw, H.M., Franke, L., Saris, C.G., Van den Bosch, L., de Jong, S.W., de Jong, V., Baas, F., van't Slot, R. *et al.* (2008) Genetic variation in DPP6 is associated with susceptibility to amyotrophic lateral sclerosis. *Nat. Genet.*, **40**, 29–31.
34. van Es, M.A., Veldink, J.H., Saris, C.G., Blauw, H.M., van Vught, P.W., Birve, A., Lemmens, R., Schelhaas, H.J., Groen, E.J., Huisman, M.H. *et al.* (2009) Genome-wide association study identifies 19p13.3 (UNC13A) and 9p21.2 as susceptibility loci for sporadic amyotrophic lateral sclerosis. *Nat. Genet.*, **41**, 1083–1087.
35. Landers, J.E., Melki, J., Meininger, V., Glass, J.D., van den Berg, L.H., van Es, M.A., Sapp, P.C., van Vught, P.W., McKenna-Yasek, D.M., Blauw, H.M. *et al.* (2009) Reduced expression of the Kinesin-Associated Protein 3 (KIFAP3) gene increases survival in sporadic amyotrophic lateral sclerosis. *Proc. Natl Acad. Sci. USA*, **106**, 9004–9009.
36. Fernandez-Santiago, R., Sharma, M., Berg, D., Illig, T., Anneser, J., Meyer, T., Ludolph, A. and Gasser, T. (2009) No evidence of association of FLJ10986 and ITPR2 with ALS in a large German cohort. *Neurobiol. Aging*, **32**, 551e1–551e4.
37. Fogh, I., D'Alfonso, S., Gellera, C., Ratti, A., Cereda, C., Penco, S., Corrado, L., Soraru, G., Castellotti, B., Tiloca, C. *et al.* (2009) No association of DPP6 with amyotrophic lateral sclerosis in an Italian population. *Neurobiol. Aging*, **32**, 966–967.
38. Chiò, A., Schymick, J.C., Restagno, G., Scholz, S.W., Lombardo, F., Lai, S.L., Mora, G., Fung, H.C., Britton, A., Arepalli, S. *et al.* (2009) A two-stage genome-wide association study of sporadic amyotrophic lateral sclerosis. *Hum. Mol. Genet.*, **18**, 1524–1532.
39. Daoud, H., Belzil, V., Desjarlais, A., Camu, W., Dion, P.A. and Rouleau, G.A. (2010) Analysis of the UNC13A gene as a risk factor for sporadic amyotrophic lateral sclerosis. *Arch. Neurol.*, **67**, 516–517.
40. Laaksovirta, H., Peuralinna, T., Schymick, J.C., Scholz, S.W., Lai, S.L., Myllykangas, L., Sulkava, R., Jansson, L., Hernandez, D.G., Gibbs, J.R. *et al.* (2010) Chromosome 9p21 in amyotrophic lateral sclerosis in Finland: a genome-wide association study. *Lancet Neurol.*, **9**, 978–985.
41. Shatunov, A., Mok, K., Newhouse, S., Weale, M.E., Smith, B., Vance, C., Johnson, L., Veldink, J.H., van Es, M.A., van den Berg, L.H. *et al.* (2010) Chromosome 9p21 in sporadic amyotrophic lateral sclerosis in the UK and seven other countries: a genome-wide association study. *Lancet Neurol.*, **9**, 986–994.
42. Iida, A., Takahashi, A., Deng, M., Zhang, Y., Wang, J., Atsuta, N., Tanaka, F., Kamei, T., Sano, M., Oshima, S. *et al.* (2011) Replication analysis of SNPs on 9p21.2 and 19p13.3 with amyotrophic lateral sclerosis in East Asians. *Neurobiol. Aging*, **32**, 757e13–757e14.
43. Haga, H., Yamada, R., Ohnishi, Y., Nakamura, Y. and Tanaka, T. (2002) Gene-based SNP discovery as part of the Japanese Millennium Genome Project: identification of 190,562 genetic variations in the human genome. Single-nucleotide polymorphism. *J. Hum. Genet.*, **47**, 605–610.
44. Henrich-Noack, P., Prehn, J.H. and Krieglstein, J. (1994) Neuroprotective effects of TGF-beta 1. *J. Neural. Transm. Suppl.*, **43**, 33–45.
45. Iwasaki, Y., Shiojima, T., Tagaya, N., Kobayashi, T. and Kinoshita, M. (1997) Effect of transforming growth factor beta 1 on spinal motor neurons after axotomy. *J. Neurol. Sci.*, **147**, 9–12.
46. Krieglstein, K., Strelau, J., Schober, A., Sullivan, A. and Unsicker, K. (2002) TGF-beta and the regulation of neuron survival and death. *J. Physiol. Paris*, **96**, 25–30.
47. Ozaki, K., Ohnishi, Y., Iida, A., Sekine, A., Yamada, R., Tsunoda, T., Sato, H., Hori, M., Nakamura, Y. and Tanaka, T. (2002) Functional SNPs in the lymphotoxin-alpha gene that are associated with susceptibility to myocardial infarction. *Nat. Genet.*, **32**, 650–654.
48. Kubo, M., Hata, J., Ninomiya, T., Matsuda, K., Yonemoto, K., Nakano, T., Matsushita, T., Yamazaki, K., Ohnishi, Y., Saito, S. *et al.* (2007) A nonsynonymous SNP in PRKCH (protein kinase C eta) increases the risk of cerebral infarction. *Nat. Genet.*, **39**, 212–217.
49. Tomlinson, I.P., Webb, E., Carvajal-Carmona, L., Broderick, P., Howarth, K., Pittman, A.M., Spain, S., Lubbe, S., Walther, A., Sullivan, K. *et al.* (2008) A genome-wide association study identifies colorectal cancer susceptibility loci on chromosomes 10p14 and 8q23.3. *Nat. Genet.*, **40**, 623–630.
50. Miyamoto, Y., Shi, D., Nakajima, M., Ozaki, K., Sudo, A., Kotani, A., Uchida, A., Tanaka, T., Fukui, N., Tsunoda, T. *et al.* (2008) Common variants in DVWA on chromosome 3p24.3 are associated with susceptibility to knee osteoarthritis. *Nat. Genet.*, **40**, 994–998.
51. Suppiah, V., Moldovan, M., Ahlenstiel, G., Berg, T., Weltman, M., Abate, M.L., Bassendine, M., Spengler, U., Dore, G.J., Powell, E. *et al.* (2009) IL28B is associated with response to chronic hepatitis C interferon-alpha and ribavirin therapy. *Nat. Genet.*, **41**, 1100–1104.
52. Price, A.L., Patterson, N.J., Plenge, R.M., Weinblatt, M.E., Shadick, N.A. and Reich, D. (2006) Principal components analysis corrects for stratification in genome-wide association studies. *Nat. Genet.*, **38**, 904–909.
53. Weir, B.S. (1996) *Genetic Data Analysis II.* Sinauer Associates, Sunderland.
54. Colland, F., Jacq, X., Trouplin, V., Mougin, C., Groizeleau, C., Hamburger, A., Meil, A., Wojcik, J., Legrain, P. and Gauthier, J.M. (2004) Functional proteomics mapping of a human signaling pathway. *Genome Res.*, **14**, 1324–1332.
55. Zawel, L., Dai, J.L., Buckhaults, P., Zhou, S., Kinzler, K.W., Vogelstein, B. and Kern, S.E. (1998) Human Smad3 and Smad4 are sequence-specific transcription activators. *Mol. Cell*, **1**, 611–617.
56. Nagase, T., Ishikawa, K., Kikuno, R., Hirosawa, M., Nomura, N. and Ohara, O. (1999) Prediction of the coding sequences of unidentified human genes. XV. The complete sequences of 100 new cDNA clones from brain which code for large proteins in vitro. *DNA Res.*, **6**, 337–345.
57. Docagne, F., Nicole, O., Gabriel, C., Fernandez-Monreal, M., Lesne, S., Ali, C., Plawinski, L., Carmeliet, P., MacKenzie, E.T., Buisson, A. *et al.* (2002) Smad3-dependent induction of plasminogen activator inhibitor-1 in astrocytes mediates neuroprotective activity of transforming growth factor-beta 1 against NMDA-induced necrosis. *Mol. Cell Neurosci.*, **21**, 634–644.
58. Houi, K., Kobayashi, T., Kato, S., Mochio, S. and Inoue, K. (2002) Increased plasma TGF-beta1 in patients with amyotrophic lateral sclerosis. *Acta Neurol. Scand.*, **106**, 299–301.
59. Jiang, Y.M., Yamamoto, M., Kobayashi, Y., Yoshihara, T., Liang, Y., Terao, S., Takeuchi, H., Ishigaki, S., Katsuno, M., Adachi, H. *et al.* (2005) Gene expression profile of spinal motor neurons in sporadic amyotrophic lateral sclerosis. *Ann. Neurol.*, **57**, 236–251.
60. Nakamura, M., Ito, H., Wate, R., Nakano, S., Hirano, A. and Kusaka, H. (2008) Phosphorylated Smad2/3 immunoreactivity in sporadic and familial amyotrophic lateral sclerosis and its mouse model. *Acta Neuropathol.*, **115**, 327–334.
61. Ilzecka, J., Stelmasiak, Z. and Dobosz, B. (2002) Transforming growth factor-Beta 1 (tgf-Beta 1) in patients with amyotrophic lateral sclerosis. *Cytokine*, **20**, 239–243.
62. Brooks, B.R., Miller, R.G., Swash, M. and Munsat, T.L. (2000) El Escorial revisited: revised criteria for the diagnosis of amyotrophic lateral sclerosis. *Amyotroph. Lateral Scler. Other Motor Neuron Disord.*, **1**, 293–299.
63. Nakamura, Y. (2007) The BioBank Japan Project. *Clin. Adv. Hematol. Oncol.*, **5**, 696–697.
64. Ohnishi, Y., Tanaka, T., Ozaki, K., Yamada, R., Suzuki, H. and Nakamura, Y. (2001) A high-throughput SNP typing system for genome-wide association studies. *J. Hum. Genet.*, **46**, 471–477.
65. Tsunoda, T., Lathrop, G.M., Sekine, A., Yamada, R., Takahashi, A., Ohnishi, Y., Tanaka, T. and Nakamura, Y. (2004) Variation of gene-based SNPs and linkage disequilibrium patterns in the human genome. *Hum. Mol. Genet.*, **13**, 1623–1632.
66. Saito, A. and Kamatani, N. (2002) Strategies for genome-wide association studies: optimization of study designs by the stepwise focusing method. *J. Hum. Genet.*, **47**, 360–365.
67. International HapMap Consortium. (2005) A haplotype map of the human genome. *Nature*, **437**, 1299–1320.
68. Andrews, N.C. and Faller, D.V. (1991) A rapid micropreparation technique for extraction of DNA-binding proteins from limiting numbers of mammalian cells. *Nucleic Acids Res.*, **19**, 2499.

ELSEVIER

Neurobiology of Aging 32 (2011) 757.e13–757.e14

NEUROBIOLOGY OF AGING

www.elsevier.com/locate/neuaging

Negative results

Replication analysis of SNPs on 9p21.2 and 19p13.3 with amyotrophic lateral sclerosis in East Asians

Aritoshi Iida[a], Atsushi Takahashi[b], Min Deng[c], Yun Zhang[c], Jing Wang[c], Naoki Atsuta[d], Fumiaki Tanaka[d], Tetsumasa Kamei[e], Motoki Sano[f], Shuichi Oshima[g], Torao Tokuda[h], Mitsuya Morita[i], Chizuru Akimoto[i], Masahiro Nakajima[a], Michiaki Kubo[j], Naoyuki Kamatani[b], Imaharu Nakano[i], Gen Sobue[d], Yusuke Nakamura[k,l], Dongsheng Fan[c,**], Shiro Ikegawa[a,*]

[a] *Laboratory for Bone and Joint Diseases, Center for Genomic Medicine, RIKEN, Tokyo, Japan*
[b] *Laboratory for Statistical Analysis, Center for Genomic Medicine, RIKEN, Tokyo, Japan*
[c] *Department of Neurology, Peking University Third Hospital, Beijing, China*
[d] *Department of Neurology, Graduate School of Medicine, Nagoya University, Aichi, Japan*
[e] *Department of Neurology, Chigasaki Tokushukai General Hospital, Kanagawa, Japan*
[f] *Department of Neurology, Chibanishi General Hospital, Chiba, Japan*
[g] *Department of Neurosurgery, Chiba Tokushukai Hospital, Chiba, Japan*
[h] *Tokushukai Group, Tokyo, Japan*
[i] *Division of Neurology, Department of Medicine, Jichi Medical University, Tochigi, Japan*
[j] *Laboratory for Genotyping Development, Center for Genomic Medicine, RIKEN, Kanagawa, Japan*
[k] *Laboratory for International Alliance, Center for Genomic Medicine, RIKEN, Kanagawa, Japan*
[l] *Laboratory of Molecular Medicine, Human Genome Center, Institute of Medical Science, The University of Tokyo, Tokyo, Japan*

Received 29 September 2010; received in revised form 11 December 2010; accepted 21 December 2010

Abstract

We performed a replication study of the 2 genetic variants, rs2814707 on 9p21.2 and rs12608932 on 19p13.3 that are recently reported to be most significantly associated with sporadic amyotrophic lateral sclerosis (ALS) in Caucasians. Both rs12608932 and rs2814707 showed no evidence of association in Japanese and Chinese (rs12608932, combined $p = 0.58$, odds ratio [OR] = 1.03, 95% confidence interval [CI] 0.93–1.13; rs2814707, combined $p = 0.88$, OR = 1.10, 95% CI 0.93–1.30). The association of these loci with susceptibility to sporadic ALS is considered negative in East Asians.

Keywords: Amyotrophic lateral sclerosis; Single nucleotide polymorphism; Genome-association study; Replication study; UNC13A; 9p21.2

Recently, van Es et al. (2009) identified 2 loci significantly associated with sporadic amyotrophic lateral sclerosis (ALS) in Caucasians. The genome-wide level association was identified on 3 single nucleotide polymorphisms (SNPs), in the order of significance, rs12608932 on chromosome 19p13.3 and rs2814707 and rs3849942 on chromosome 9p21.2. In this study, we checked replication of the association of the 2 loci in Japanese (1179 cases and 1645 controls) and Chinese (684 cases and 830 controls) cohorts by examining the most significantly associated SNPs (rs12608932 and rs2814707) in the previous study (van Es et al., 2009). Detailed materials and methods are described in Supplementary data.

* Corresponding author at: Laboratory for Bone and Joint Diseases, Center for Genomic Medicine, RIKEN, Institute of Medical Science, The University of Tokyo, 4-6-1 Shirokanedai, Minato-ku, Tokyo 108-8639, Japan. Tel.: +81 3 5449 5393; fax: +81 3 5449 5393.
E-mail address: sikegawa@ims.u-tokyo.ac.jp (S. Ikegawa).
** Alternate corresponding author at: Department of Neurology, Peking University Third Hospital, 49 North Garden Road, Haidian District, Beijing 100191, China.
E-mail address: dsfan@yahoo.cn (D. Fan).

0197-4580/$ – see front matter © 2011 Elsevier Inc. All rights reserved.
doi:10.1016/j.neurobiolaging.2010.12.011

The allele frequency of rs12608932 was different between Caucasians and East Asians (Supplementary Table 1). The association in Japanese did not reach statistical significance by a logistic regression analysis (p = 0.67, odds ratio [OR] = 1.02, 95% confidence interval [CI] 0.91–1.16). Similarly, no association of rs12608932 with sporadic ALS was detected in Chinese (p = 0.73, OR = 1.02, 95% CI 0.88–1.20). We then calculated combined p value for the Japanese and Chinese studies by an inverse variance method and observed no association in the East Asians (p = 0.58, OR = 1.03, 95% CI 0.93–1.13).

We found that rs2814707 was not associated with susceptibility to sporadic ALS in Japanese and Chinese (Supplementary Table 1). The meta-analysis showed that there was no evidence for the association between rs2814707 and risk of sporadic ALS in East Asians (p = 0.88, OR = 1.10, 95% CI 0.93–1.30). However, because the power of the study was less than 80%, this negative association may be due to lack of power that resulted from the limited sample size and/or low risk allele frequency in East Asians. The association between rs2814707 and sporadic ALS in East Asians requires confirmation in further replication studies.

Appendix A. Supplementary data

Supplementary data associated with this article can be found, in the online version, at doi:10.1016/j.neurobiolaging.2010.12.011.

Reference

van Es, M.A., Veldink, J.H., Saris, C.G., Blauw, H.M., van Vught, P.W., Birve, A., Lemmens, R., Schelhaas, H.J., Groen, E.J., Huisman, M.H., van der Kooi, A.J., de Visser, M., Dahlberg, C., Estrada, K., Rivadeneira, F., Hofman, A., Zwarts, M.J., van Doormaal, P.T., Rujescu, D., Strengman, E., Giegling, I., Muglia, P., Tomik, B., Slowik, A., Uitterlinden, A.G., Hendrich, C., Waibel, S., Meyer, T., Ludolph, A.C., Glass, J.D., Purcell, S., Cichon, S., Nöthen, M.M., Wichmann, H.E., Schreiber, S., Vermeulen, S.H., Kiemeney, L.A., Wokke, J.H., Cronin, S., McLaughlin, R.L., Hardiman, O., Fumoto, K., Pasterkamp, R.J., Meininger, V., Melki, J., Leigh, P.N., Shaw, C.E., Landers, J.E., Al-Chalabi, A., Brown, R.H., Jr, Robberecht, W., Andersen, P.M., Ophoff, R.A., van den Berg, L.H., 2009. Genome-wide association study identifies 19p13.3 (UNC13A) and 9p21.2 as susceptibility loci for sporadic amyotrophic lateral sclerosis. Nat. Genet. 41, 1083–1087.

Neurobiology of Disease 45 (2012) 862–870

Contents lists available at SciVerse ScienceDirect

Neurobiology of Disease

journal homepage: www.elsevier.com/locate/ynbdi

Oxidative stress induced by glutathione depletion reproduces pathological modifications of TDP-43 linked to TDP-43 proteinopathies

Yohei Iguchi [a], Masahisa Katsuno [a], Shinnosuke Takagi [a], Shinsuke Ishigaki [a,d], Jun-ichi Niwa [b], Masato Hasegawa [c], Fumiaki Tanaka [a], Gen Sobue [a,d,*]

[a] Department of Neurology, Nagoya University Graduate School of Medicine, 65 Tsurumai-cho, Showa-ku, Nagoya 466–8550, Japan
[b] Stroke Center, Aichi Medical University, Aichi 480–1195, Japan
[c] Departments of Molecular Neurobiology, Tokyo Institute of Psychiatry, Tokyo Metropolitan Organization for Medical Research, 2-1-8 Kamikitazawa, Setagaya-ku, Tokyo 156–8585, Japan
[d] CREST, Japan Science and Technology Agency, 4-1-8, Honcho, Kawaguchi, Saitama 332–0012, Japan

ARTICLE INFO

Article history:
Received 30 March 2011
Revised 29 August 2011
Accepted 4 December 2011
Available online 13 December 2011

Keywords:
TAR DNA-binding protein 43 kDa (TDP-43)
TDP-43 proteinopathy
Oxidative stress
Glutathione depletion
Post-translational modification
Protein phosphorylation

ABSTRACT

TAR DNA-binding protein 43 (TDP-43) is a major component of ubiquitin-positive inclusion of TDP-43 proteinopathies including amyotrophic lateral sclerosis and frontotemporal lobar degeneration with ubiquitinated inclusions, which is now referred to as FTLD-TDP. TDP-43 in the aberrant inclusion is known to be hyperphosphorylated at C-terminal sites, to be truncated at the N-terminal region, and to re-distribute from nucleus to cytoplasm or neurite. The pathogenic role of these modifications, however, has not been clarified. Furthermore, there is no evidence about the initial cause of these modifications. Herein we show that ethacrynic acid (EA), which is able to increase cellular oxidative stress through glutathione depletion, induces TDP-43 C-terminal phosphorylation at serine 403/404 and 409/410, insolubilization, C-terminal fragmentation, and cytoplasmic distribution in NSC34 cells and primary cortical neurons. In the investigation using a nonphosphorylable mutant of TDP-43, there was no evidence that C-terminal phosphorylation of TDP-43 contributes to its solubility or distribution under EA induction. Our findings suggest that oxidative stress induced by glutathione depletion is associated with the process of the pathological TDP-43 modifications and provide new insight for TDP-43 proteinopathies.

Introduction

TAR DNA-binding protein 43 (TDP-43) is a major component of ubiquitin-positive inclusion, a pathological hallmark of TDP-43 proteinopathies including amyotrophic lateral sclerosis (ALS) and frontotemporal lobar degeneration with ubiquitinated inclusions, which is now referred to as FTLD-TDP (Arai et al., 2006; Neumann et al., 2006). Both diseases occur in sporadic or familial forms, and are characterized by late-onset progressive deterioration of motor and/or cognitive function. TDP-43 is a heterogeneous nuclear ribonucleoprotein (hnRNP), which is known to regulate gene transcription and exon splicing through interactions with RNA, hnRNPs, and nuclear bodies (Ayala et al., 2005; Buratti et al., 2005; Wang et al., 2002, 2004). In addition, this protein has also been reported to stabilize human low molecular weight neurofilament (hNFL) mRNA through direct interaction with its 3'UTR (Strong et al., 2007), regulate retinoblastoma protein phosphorylation through the repression of cyclin-dependent kinase 6 (Cdk6) expression (Ayala et al., 2008), regulate activity of Rho family GTPases (Iguchi et al., 2009), and alter the expression of selected microRNAs, such as let-7b and miR-663 (Buratti et al., 2010). Furthermore, very recent works using cross-linking immunoprecipitation sequencing show that multiple RNAs interact with TDP-43 (Polymenidou et al., 2011; Sephton et al., 2011; Tollervey et al., 2011).

Although it mostly localizes in the nucleus under normal conditions, TDP-43 is distributed from nucleus to cytoplasm or neurite, and forms aggregates consisting mainly of C-terminal fragments in affected neurons of patients with TDP-43 proteinopathies. In addition, TDP-43 in the aberrant aggregation is hyperphosphorylated at multiple C-terminal sites (Hasegawa et al., 2008). However, neither the pathogenic role nor the initial cause of these abnormal modifications of TDP-43 has been elucidated. The fact that the majority of patients with TDP-43 proteinopathies are sporadic suggests that exogenous factors induce post-translational modifications of TDP-43 that are seen in the disease. Furthermore, TDP-43 inclusions have also been observed in Alzheimer disease (AD), Parkinson disease (PD),

Abbreviations: TDP-43, TAR DNA-binding protein of 43 kDa; ALS, amyotrophic lateral sclerosis; hnRNP, heterogeneous nuclear ribonucleoprotein; hNFL, human low molecular weight neurofilament; Cdk6, cyclin-dependent kinase 6; ROS, reactive oxygen species; EA, ethacrynic acid; NAC, N-acetylcysteine; CK1, casein kinase 1; CK2, casein kinase 2; WT-TDP-43, wild type TDP-43; SA-TDP-43, nonphosphorylable TDP-43.

* Corresponding author at: Department of Neurology, Nagoya University Graduate School of Medicine, 65 Tsurumai-cho, Showa-ku, Nagoya 466–8550, Japan. Fax: +81 52 744 2785.
E-mail address: sobueg@med.nagoya-u.ac.jp (G. Sobue).

Available online on ScienceDirect (www.sciencedirect.com).

0969-9961/$ – see front matter © 2011 Elsevier Inc. All rights reserved.
doi:10.1016/j.nbd.2011.12.002

dementia with Lewy bodies (DLB), and Huntington disease (HD), argyrophilic grain disease, suggesting that the aggregation of this protein may be a secondary feature of neurodegeneration (Amador-Ortiz et al., 2007; Arai et al., 2009, 2010; Geser et al., 2008; Hasegawa et al., 2007). These findings complicate understanding of the pathogenic role of TDP-43. On the other hand, there is considerable evidence that reactive oxygen species (ROS) and oxidative stress are associated with many neurodegenerative conditions including ALS (Abe et al., 1995, 1997; Beal et al., 1997; Butterfield et al., 2007; Ferrante et al., 1997; Lovell and Markesbery, 2007; Nunomura et al., 2002; Shaw et al., 1995). Herein we show that oxidative stress induced by glutathione depletion reproduces the pathological modifications of TDP-43, that are seen in TDP-43 proteinopathies, in motor neuron-like cells and primary cortical neurons.

Materials and methods

Cell culture and treatment

Mouse NSC34 motor neuron-like cells (a kind gift of N.R. Cashman, University of British Columbia, Vancouver, Canada) were cultured in a humidified atmosphere of 95% air-5% CO2 in a 37 °C incubator in Dulbecco's Modified Eagle's Medium (DMEM) supplemented with 10% fetal bovine serum (FBS). To differentiate the cells, the medium was changed to DMEM containing 1% FBS and 1% NEAA, and was cultured for 24 h. For the interventions, the cells were then incubated with ethacrynic acid (EA) (Sigma-Aldrich, St. Louis, MO), with or without N-acetylcysteine (NAC) (Sigma-Aldrich), casein kinase 1 (CK1) inhibitor (D4476), or casein kinase 2 (CK2) inhibitor (TBCA) (Sigma-Aldrich). Primary cultures of mouse embryonic cortical neurons that were dissociated from embryonic cortex of embryonic day 15 (E15) C57BL/6 J pregnant mice were plated onto poly-L-lysine-coated plates or glass bottom dishes, and maintained in neuron culture medium (Sumilon, Osaka, Japan). Five days after the incubation, the indicated interventions were performed. In both NSC34 cells and primary cortical neurons, the transfections of the intended plasmids were performed using Lipofectamine 2000 (Invitrogen, Eugene, OR), according to the manufacturer's instructions.

DNA constructs

Human wild type TDP-43 (WT-TDP-43) (accession number NM 007375) cDNA was amplified by PCR from cDNA of human spinal cord using the following primers: 5′-CACCATGTCTGAATATATTCGGGTAAC-3′ and 5′-CTACATTCCCCAGCCAGAAGACTTAGAAT-3′. The PCR product was cloned into the pENTR/D-TOPO vector (Invitrogen). For nonphosphorylable TDP-43 (SA-TDP-43) vector, primers containing the mutant substitution of TDP-43 serine 403/404 and 409/410 to alanine were used to mutagenize WT-TDP-43 (KOD-Plus-Mutagenesis kit; Toyobo, Osaka, Japan). The entry vector of WT- or SA-TDP-43 was transferred into pcDNA6.2/N-EmGFP-DEST Vector or pcDNA3.1/nV5-DEST using Gateway LR Clonase II enzyme mix (Invitrogen). The sequences of all constructs were verified using CEQ 8000 genetic analysis system (Beckman Coulter, Brea, CA).

Immunoblot analysis

For whole lysate analysis, NSC34 cells and primary cortical neurons were lysed in 2% SDS sample buffer. For analysis of protein solubility, cells cultured in 6-well plates were lysed in 100 μl of Tris (TS) buffer (50 mM Tris–HCl buffer, pH 7.5, 0.15 M NaCl, 5 mM EDTA, 5 mM EGTA, protein phosphatase inhibitors, and protease inhibitor cocktail). Lysates were sonicated and centrifuged at 100,000 ×*g* for 15 min. To prevent carryover, the pellets were washed with TS buffer, followed by sonication and centrifugation. TS-insoluble pellets were lysed in 50 μl of Triton-X100 (TX) buffer (TS buffer containing 1% Triton X-100), sonicated, and centrifuged at 100,000 *g* for 15 min. The pellets were washed with TX buffer, followed by sonication and centrifuge. TX-insoluble pellets were lysed in 50 μl of Sarkosyl (Sar) buffer (TS buffer containing 1% Sarkosyl), sonicated and centrifuged at 100,000 × g for 15 min. Sar-insoluble pellets were lysed in 25 μl of SDS sample buffer. After denaturation, 3 μl of each cell lysate was separated by SDS-PAGE (5%–20% gradient gel) and analyzed by western blotting with ECL Plus detection reagents (GE Healthcare, Buckinghamshire, UK). Primary antibodies used were as follows: anti-TDP-43 rabbit polyclonal antibody (1:1000, ProteinTech, Chicago, IL), anti-TDP-43 (405–414) rabbit polyclonal antibody (1:1000, Cosmo Bio Co. Ltd., Tokyo, Japan), anti-TDP-43 (phospho Ser403/404, Cosmo Bio) rabbit polyclonal antibody (1:1000, Cosmo Bio), anti-TDP-43 (phospho Ser409/410, Cosmo Bio) rabbit polyclonal antibody (1:1000, Cosmo Bio), anti-GAPDH mouse monoclonal antibody (1:2000, Temecula, CA), anti-GFP mouse monoclonal antibody (1:2000, MBL, Nagoya, Japan), and anti-V5 mouse monoclonal antibody (1:2000, Invitrogen).

Assay of ROS production

NSC34 cells to be treated with intended agents were incubated in 96-well plates with 5-(and-6)-chloromethyl-2′,7′-dichlorodihydro fluoresceindiacetate acetyl ester (CM-H2DCFDA) (Molecular Probes, Eugene, OR, USA) for 1 h. Oxidation in the cells was then measured in a multiple-plate reader (PowerscanHT, Dainippon Pharmaceutical, Japan) at excitation and emission wavelengths of 485 nm and 530 nm, respectively. The assays were carried out in 6 wells for each condition.

Immunocytochemistry

NSC34 cells and primary cortical neurons were fixed with 4% paraformaldehyde, incubated with PBS containing 0.2% Triton X-100 for 5 min, blocked, and incubated overnight with anti-TDP-43 rabbit polyclonal antibody (1:1000, ProteinTech), anti-TDP-43 (phospho Ser409/410) mouse monoclonal antibody (1:2000, Cosmo Bio) and anti-TIAR mouse monoclonal antibody (1:1000, BD Transduction Laboratories, Milan, Italy). After washing, samples were incubated with Alexa-488-conjugated goat anti-rabbit IgG (1:1000, Invitrogen) and Alexa-564-conjugated goat anti-mouse IgG (1:1000, Invitrogen) for 30 min, mounted with (Vector Laboratories, Inc. Burlingame, CA), then imaged with a laser conforcal microscope (Nikon A1, Nikon, Tokyo, Japan).

Time lapse analysis

NSC34 cells or mouse primary cortical neurons were grown on glass base dishes, transfected with GFP-WT-TDP-43, and treated with EA. GFP and phase contrast imaging was done every 10 min using a 40X objective lens on a laser scanning confocal microscope.

Cell viability analysis

The 3-(4,5-dimethylthiazol-2-yl)-5-(3-caboxymethoxyphenyl)-2-(4-sulfophenyl)-2H -tetrazolium (MTS)-based cell proliferation assay (MTS assay) was carried out using the CellTiter 96 Aqueous One Solution Cell Proliferation Assay (Promega, Madison, WI), according to the manufacturer's instructions. Absorbance at 490 nm was measured in a multiple-plate reader (PowerscanHT, Dainippon Pharmaceutical, Japan). The assays were carried out in 6 wells for each condition.

Statistical analysis

Statistical differences were analyzed by ANOVA and Bonferroni post hoc analyses for three group comparisons (SPSS version 15.0, SPSS Inc., Chicago, IL). Two-tailed $p<0.05$ was regarded as statistically significant.

Results

EA-mediated oxidative stress induces TDP-43 phosphorylation in NSC34 cells

To investigate the effect of oxidative stress on endogenous TDP-43, NSC34 cells were incubated for 12 h with EA, which is able to increase cellular oxidative stress through depletion of glutathione, (Keelan et al., 2001; Rizzardini et al., 2003). Immunoblots showed abnormal TDP-43-immunoreactive bands at 45 kDa, which suggests hyperphosphorylation of TDP-43, at EA concentration greater than 50 μM EA (Fig. 1A). The bands were immunopositive for phospho-TDP-43-specific (pTDP-43) antibodies at serine 403/404 and serine 409/410 (S403/404 and S409/410), that are seen in TDP-43 proteinopathies as pathological phosphorylation (Hasegawa et al., 2008) (Fig. 1A). In addition, phosphorylation of these TDP-43 sites was prevented by co-treatment with 2 mM NAC, a precursor of glutathione. Quantification of CM-H2DCFDA oxidation, a measure of ROS formation, showed that ROS productions was increased by EA treatment in a dose-dependent manner and was prevented by NAC (Fig. 1B). Since TDP-43 phosphorylation at S403/404 and S409/410 is exerted by CK1 and CK2 (Hasegawa et al., 2008), the effect of treatment with these inhibitors in combination with EA was examined. Both inhibitors prevented serine phosphorylation of TDP-43 in a dose-dependent manner, although CK1 inhibitor was more effective than CK2 inhibitor (Fig. 1C).

EA induces TDP-43 insolubilization and C-terminal fragmentation

To investigate the effect of oxidative stress on endogenous TDP-43 solubility, cells treated with 70 μM EA were extracted sequentially. In the immunoblots, the amount of TDP-43 in TS and TX fractions were significantly decreased, but the amount in Sar and SDS fractions were increased in a time-dependent manner (Fig. 2A). These phenomena were prevented in the presence of 2 mM NAC. Phosphorylated TDP-43 was increased in Sar fractions in a time-dependent manner and was detectable in SDS fractions 5 h after EA induction (Fig. 2A). In addition, long exposure of immunoblots with anti-TDP-43 antibody demonstrated that ~25 kDa C-terminal fragment (CTF) of TDP-43 in Sar and SDS fractions appeared evidently by EA induction, and the amount of TDP-43 CTF in SDS fraction was significantly increased at 5 h after EA induction compared with control (Fig. 2A, B).

EA induces cytoplasmic distribution of TDP-43

Immunocytochemistry showed that endogenous TDP-43 disappeared from the nucleus, translocated to the cytoplasm, and became phosphorylated at least in some population of NSC34 cells treated with 70 μM EA for 5 h, whereas this protein was localized in the nucleus and was not phosphorylated in untreated cells (Fig. 3A). Although the majority of cytoplasmic TDP-43 was diffusely distributed under EA treatment, it was also localized in stress granules (SGs), which were labeled with TIAR (Fig. 3A). The time lapse analysis of NSC43 cells expressing GFP-WT-TDP-43 demonstrated cytoplasmic distribution of TDP-43 in the majority of the cells treated with 70 μM EA, but TDP-43 consistently localized in the nucleus of cells co-treated with 2 mM NAC (Fig. 3B, C).

H_2O_2 induces C-terminal phosphorylation, C-terminal fragmentation, insolubilization, and cytoplasmic distribution of TDP-43

To confirm that the TDP-43 modifications are not induced by the specific toxicity of EA, we investigated the effects of H_2O_2, another

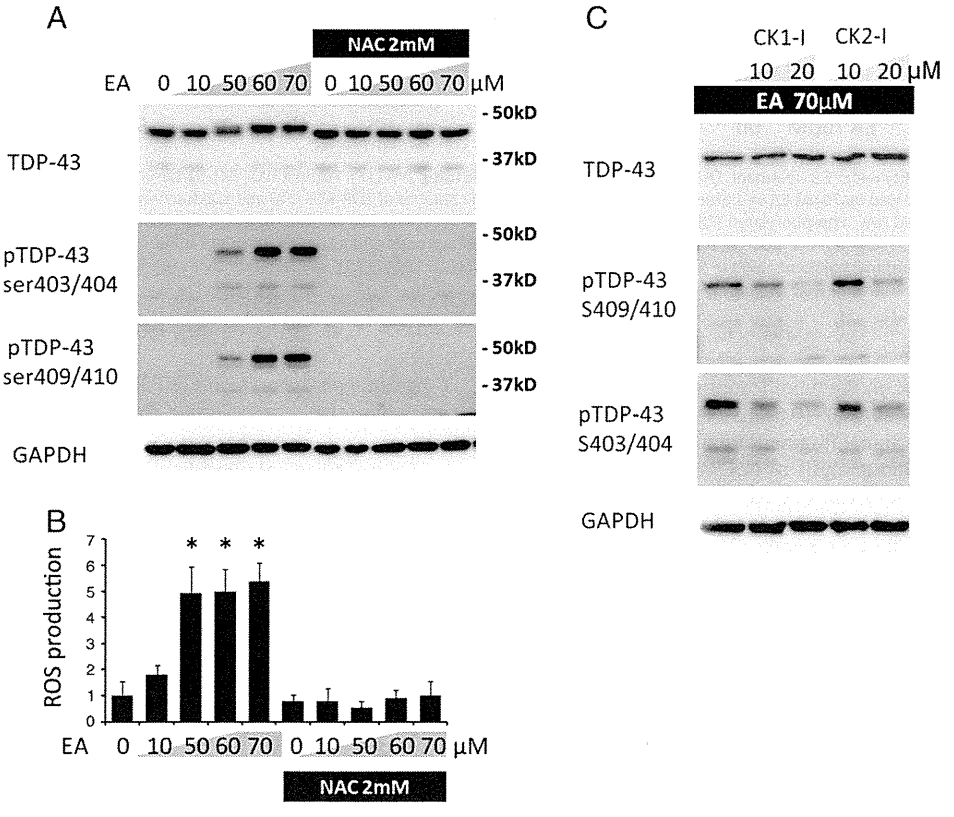

Fig. 1. TDP-43 phosphorylation induced by EA. (A) Immunoblots of NSC34 cells. EA induced TDP-43 C-terminal phosphorylation at S403/404 and S409/410 in a dose-dependent manner. The phosphorylation was prevented by 2 mM NAC. (B) Quantification of ROS by CM-H2DCFDA oxidative assay. The values relative to those of controls are shown. ROS production was increased by EA induction and suppressed by 2 mM NAC. Asterisk denotes significant difference from control ($p<0.0001$, $n=6$). Error bars indicate SD. (C) Immunoblots of NSC34 cells treated with 70 μM of EA. Casein kinase 1 and 2 inhibitors (CK1-I and CK2-I) both prevented the phosphorylation of TDP-43 in a dose-dependent manner.

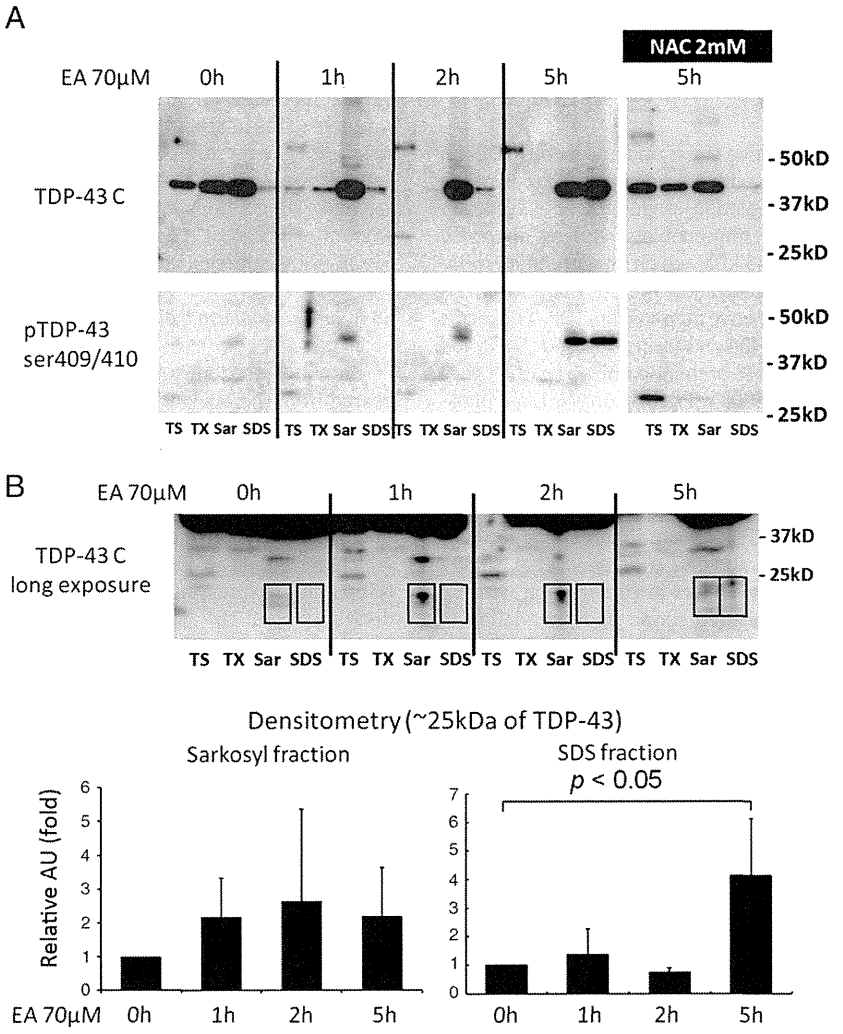

Fig. 2. Analysis of TDP-43 solubility under EA treatment. (A) Sequential extraction analysis using Tris (TS), Triton X100 (TX), Sarkosyl (Sar), and SDS buffers. The amount of TDP-43 in TS and TX fractions was decreased by 70 μM EA in a time-dependent manner, while the amount of TDP-43 in Sar and SDS fractions was increased by the treatment. These phenomena were prevented by 2 mM NAC. Phosphorylated TDP-43 (S409/410) was increased in Sar and SDS fractions in a time-dependent manner. (B) Densitometric quantitation of TDP-43C-terminal fragment (CTF). The relative intensities to controls are shown in arbitrary units (AU). Long exposure of immunoblots with anti-TDP-43 antibody (405–414) (TDP-43C) showed ~25 kDa C-terminal fragment (CTF) in Sar and SDS fractions. The amount of TDP-43 CTF was significantly increased in the SDS fraction at 5 h after EA induction ($n = 3$). Error bars indicate SD.

inducer of oxidative stress, on the modifications of TDP-43. Immunoblots of NSC34 cells showed that 10 mM H_2O_2 induced C-terminal phosphorylation and C-terminal fragmentation of TDP-43 (Fig. S4A). In the sequential extraction analysis of NSC34 cells, the amount of TDP-43 in TS and TX fractions was decreased by 10 mM H_2O_2, while that of TDP-43 in SDS fraction was increased by the treatment (Fig. S4B). The time lapse analysis of NSC34 cells expressing GFP-WT-TDP-43 showed that 10 mM H_2O_2 induced cytoplasmic distribution of TDP-43 (Fig. S4C).

EA induces C-terminal phosphorylation and cytoplasmic distribution of TDP-43 in primary cortical neurons

To investigate the effect of oxidative stress in neurons, 5-day in vivo (5 DIV) mouse primary cortical neurons were treated with EA for 5 h. Immunoblots showed that EA induced TDP-43 phosphorylation at S403/404 and S409/410 in a dose-dependent manner, and 2 mM NAC prevented the phosphorylation (Fig. 4A). In the time lapse analysis of neurons expressing GFP-WT-TDP-43, TDP-43 was distributed in the cytoplasm in the presence of 30 μM EA (Fig. 4B).

C-terminal phosphorylation of TDP-43 is not mandatory for its insolubilization or cytoplasmic distribution under EA

Since C-terminal phosphorylation of TDP-43 was accompanied by insolubilization and distribution to the cytoplasm in response to oxidative stress, we investigated the effect of C-terminal phosphorylation of TDP-43 using a nonphosphorylable TDP-43 (SA-TDP-43) mutant which contains serine to alanine substitutions at 403/404 and 409/410 (Fig. 5A). We used N-terminal tagged TDP-43, since C-terminal tagged TDP-43 was not detected by anti-pTDP-43 antibody in the immunoblots even under conditions of oxidative stress sufficient to phosphorylate endogenous TDP-43 (Fig. S1). As was seen with WT-TDP-43 under normal conditions, GFP-tagged and V5-tagged SA-TDP-43 were located in the nucleus (Fig. S2). In the immunoblots, endogenous and GFP-WT-TDP-43 were phosphorylated in the presence of 70 μM EA, but GFP-SA-TDP-43 was not phosphorylated even at an EA concentration of 70 μM (Fig. 5B). The time lapse analysis of NSC34 cells demonstrated that GFP-SA-TDP-43 translocated to the cytoplasm (Fig. 6A). The proportion of the cells with cytoplasmic distribution of TDP-43 under oxidative stress was not

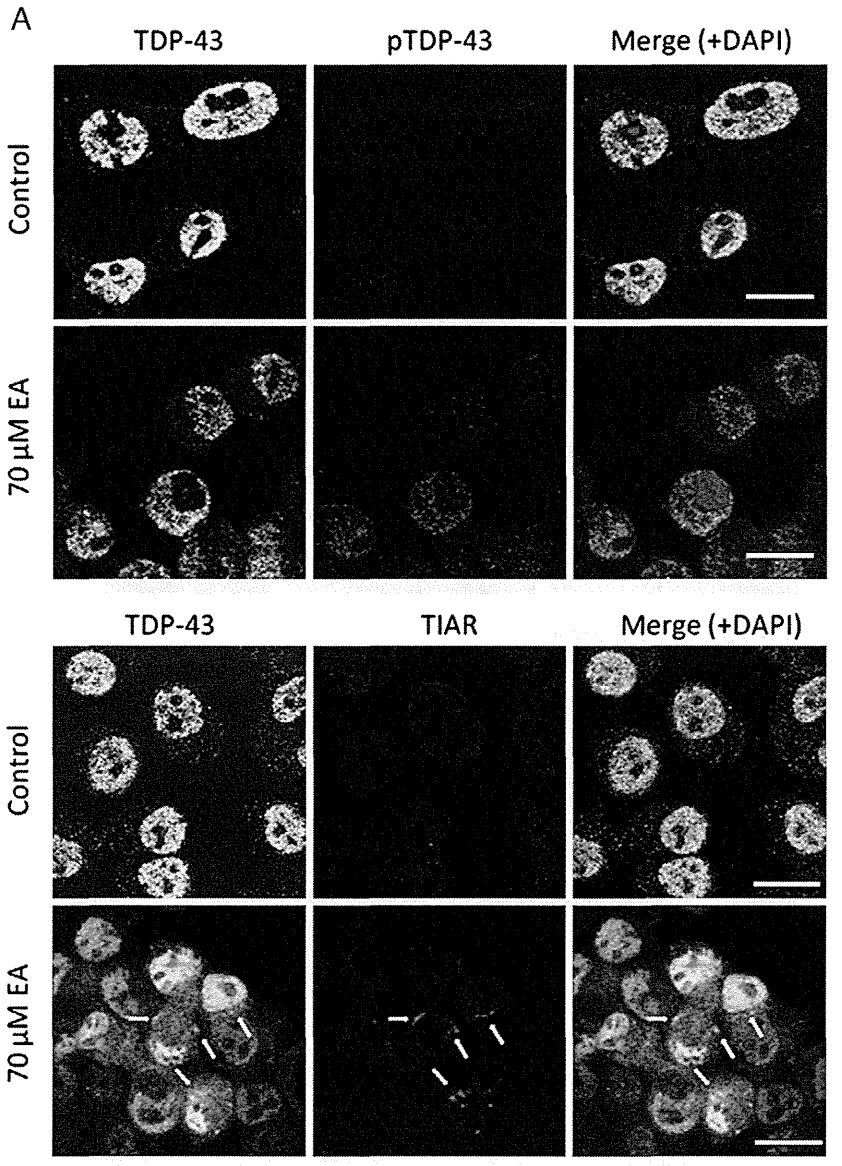

Fig. 3. Cytoplasmic distribution of TDP-43 induced by EA. (A) Immunocytochemistry of NSC34 cells. Cells were stained with anti-TDP-43 antibody (green), anti-phospho-specific TDP-43 (pTDP-43) (S409/410) or anti-TIAR antibody (red), and DAPI (blue). EA treatment (70 μM, 5 h) induced translocation of TDP-43 from the nucleus to the cytoplasm in NSC34 cells. Cytoplasmic TDP-43 was immunopositive for pTDP-43 antibody. In the control cells TDP-43 localized in the nucleus without phosphorylation. TDP-43 co-localized with stress granule marker, TIAR under EA treatment, although the majority of cytoplasmic TDP-43 was diffusely distributed. Arrows indicate stress granules. Scale bars represent 10 μm. (B) Time lapse analysis of NSC43 cells expressing GFP-WT-TDP-43. GFP and phase contrast images showed that TDP-43 was distributed to the cytoplasm when exposed to 70 μM EA, but this distribution was prevented by 2 mM of NAC. (C) The proportion of cells with cytoplasmic distribution of TDP-43 (cells with cyto-TDP) in the GFP-TDP-43 expressing cells 0 h or 5 h after EA induction without or with NAC treatment. Three areas per sample were measured. Error bars indicate SD.

different between WT- and SA-TDP-43 (Fig. 6B). Sequential extraction of NSC34 cells was performed using V5-tagged TDP-43 vectors, since the Sar-insoluble fraction of GFP-TDP-43 was abundant even in the absence of oxidative stress (data not shown). The amount of Sar-insoluble fraction of SA-TDP-43 detected was the same as was seen with WT-TDP-43. (Fig. 7A, B). These findings indicate that phosphorylation is not necessary for oxidative-stress mediated insolubilization and cytoplasmic distribution of TDP-43. Next, we performed MTS assay of NSC34 cells to investigate the effect of TDP-43 and its modifications on the cell viability. The results showed that no significant difference in the viability among the cells expressing GFP-mock, GFP-WT- and GFP-SA-TDP-43, either 0 h or 5 h after EA induction (Fig. S3).

Discussion

Post-translational modifications of TDP-43 such as C-terminal phosphorylation, insolubilization, C-terminal fragmentation, and cytoplasmic distribution are pathological hallmarks of TDP-43 proteinopathies (Arai et al., 2006; Hasegawa et al., 2008; Neumann et al., 2006). TDP-43 with defective nuclear localization signal (NLS) was shown to promote cytoplasmic aggregation, C-terminal phosphorylation, and C-terminal fragmentation of TDP-43 in cell-based studies (Nonaka et al., 2009a; Winton et al., 2008). In addition, overexpression of TDP-43 CTF lead to phosphorylation and formation of cytoplasmic aggregates (Igaz et al., 2009; Nonaka et al., 2009b). Although these observations suggest that the cytoplasmic localization

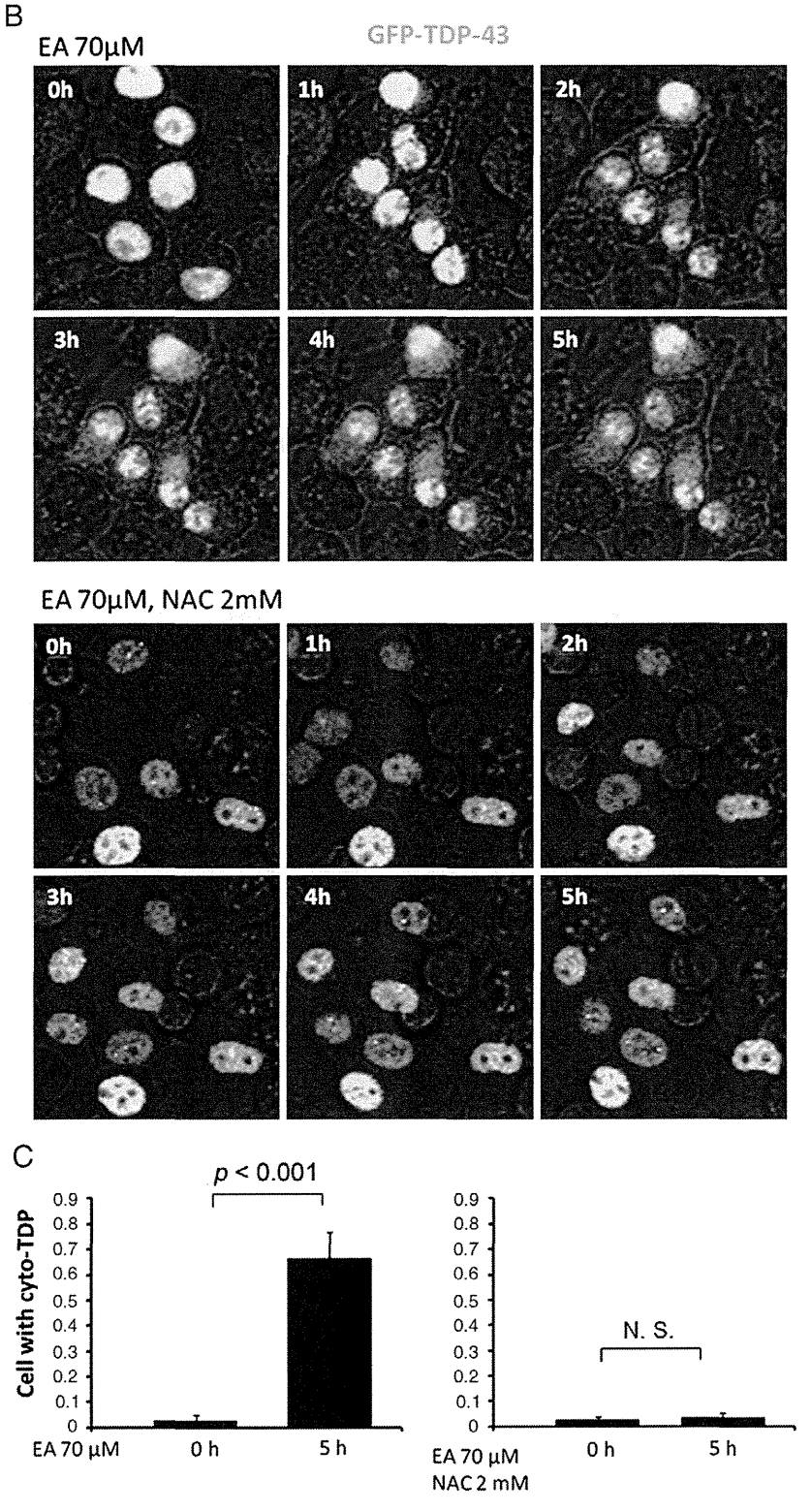

Fig. 3 (*continued*).

or fragmentation of TDP-43 facilitates its pathological modification such as aggregation and phosphorylation, the initial cause of these modifications in TDP-43 proteinopathies has not been fully elucidated. Some studies have demonstrated that artificial axonal damage induces transient cytoplasmic distribution of TDP-43 in motor neurons (Moisse et al., 2009; Sato et al., 2009), indicating that the pathological distribution of TDP-43 may result from the cellular response to neuronal injury or axonal obstruction. However, in these affected neurons, aggregation, C-terminal fragmentation and phosphorylation of TDP-43 were not observed. Furthermore, zinc-induced nuclear

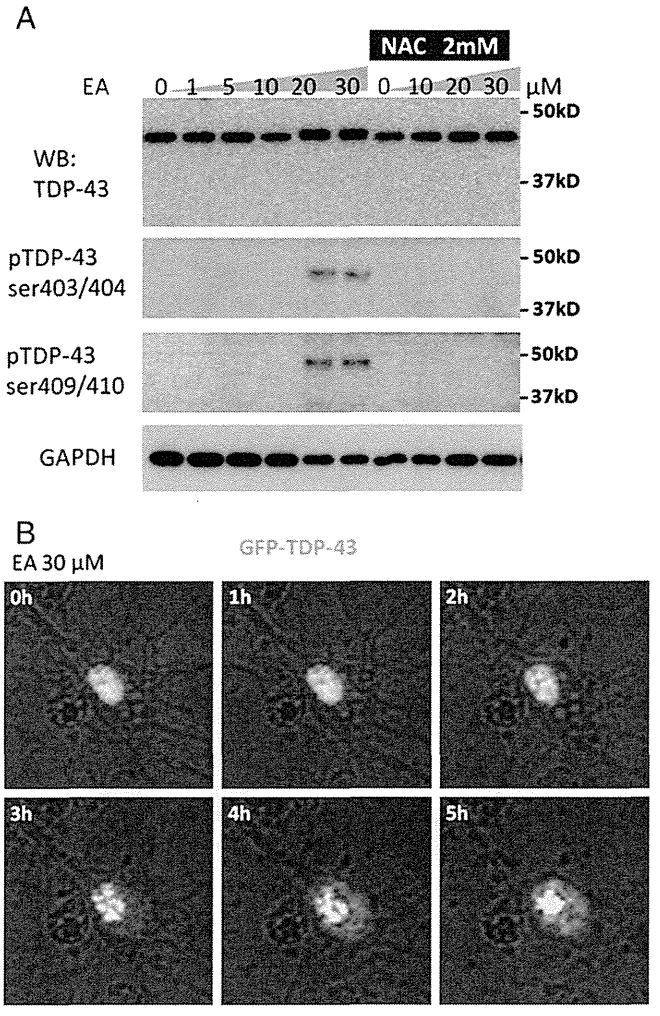

Fig. 4. TDP-43 modification induced by EA in primary cortical neuron. (A) Immunoblots of primary cortical neurons. EA induced TDP-43 phosphorylation at S403/404 and S409/410 in a dose-dependent manner, and this was prevented by 2 mM NAC. (B) Time lapse analysis of neurons expressing GFP-WT-TDP-43. TDP-43 in primary cultures was distributed to the cytoplasm in the presence of 30 μM EA.

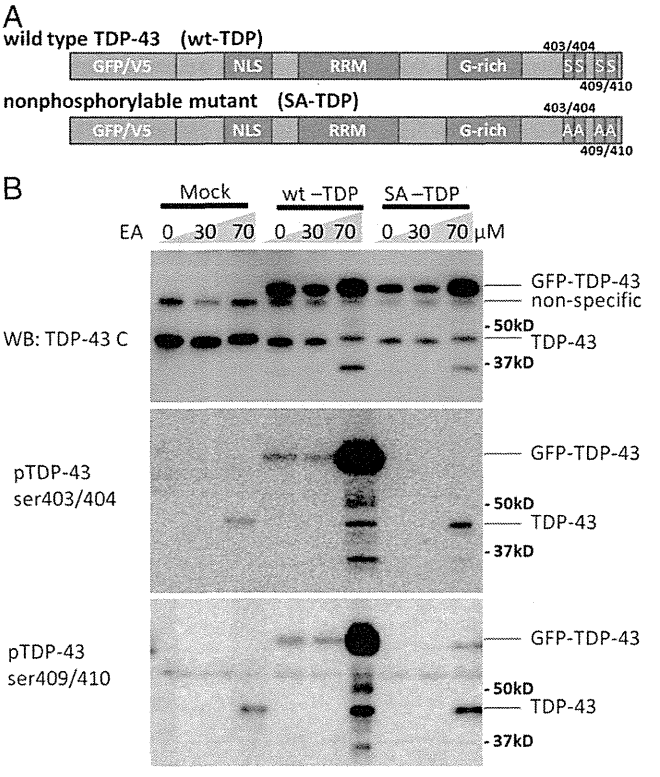

Fig. 5. Nonphosphorylable mutant of TDP-43. (A) Structures of WT- and SA-TDP-43 vectors. SA-TDP-43 contains serine to alanine substitutions at 403/404 and 409/410. (B) Immunoblots of NSC34 cells expressing GFP-WT- or GFP-SA-TDP-43. Endogenous and GFP-WT-TDP-43 were phosphorylated at both 403/404 and 409/410 by 70 μM EA, but GFP-SA-TDP-43 was not phosphorylated by the treatment.

inclusion formations have also been observed in SY5Y cells, but not C-terminal fragmentation or phosphorylation of TDP-43 (Caragounis et al., 2010).

In the present study, we demonstrated that a compound that induces cellular glutathione depletion, EA induced C-terminal phosphorylation of TPD-43 at S403/404 and S409/410 in NSC34 cells and mouse primary cortical neurons, and that NAC completely prevented this phosphorylation. In addition, inhibitors of both CK1 and CK2 also prevented the phosphorylation in a dose-dependent manner. These findings indicate that C-terminal phosphorylation of TDP-43 occurs as a consequence of oxidative stress induced by glutathione depletion and is mediated by CK1 and CK2. Furthermore, the sequential extract analysis showed that EA reduced the solubility of TDP43 and increased the amount of ~25 kDa CTF in the Sar-insoluble fraction. Additionally, EA also induced cytoplasmic distribution of TDP-43 in NSC34 cells and primary cortical neurons. The time lapse analysis showed that cytoplasmic distribution of TDP-43 was seen in the majority of NSC34 cells. Although the immunocytochemistry of TDP-43 demonstrated that cytoplasmic distribution of TDP-43 were observed only in a certain population of NSC34 cells treated with EA, this is likely due to the fact that most of damaged cells could not stay adherent to the plate during the fixation. Previous reports indicated that severe level of oxidative stress may result in apoptotic cell death, and that caspase activation induces C-terminal fragmentation of TDP-43 (Dormann et al., 2009; Zhang et al., 2007). These observations do not exclude the possibility that caspase activation contributes to TDP-43 modifications that were observed under EA treatment. The results of the present study demonstrated that H_2O_2, another inducer of oxidative stress, also causes C-terminal phosphorylation, fragmentation, insolubilization, and cytoplasmic distribution of TDP-43 as observed under EA exposure. These data suggest that oxidative stress is involved in the process of the pathological TDP-43 modifications seen in TDP-43 proteinopathies. The facts that oxidative stress is associated with aging-related disorders (Frederickson et al., 2005; Migliore, 2005) and that TDP-43 proteinopathies are aging process-related diseases may support our assumption that oxidative stress possibly mediates TDP-43 modification. A high frequency of abnormal TDP-43 pathology such as C-terminal phosphorylation has been found not only in patients with TDP-43 proteinopathies but also in patients with other neurodegenerative disease such as AD, DLB, and HD (Arai et al., 2010). Since numerous studies have demonstrated increased oxidative cellular damage in these conditions (Butterfield et al., 2007; Lovell and Markesbery, 2007; Nunomura et al., 2002), oxidative stress may be a cause of pathological TDP-43 modification in various neurodegenerative disorders.

Several studies demonstrated that TDP-43 is involved in SGs under cellular stresses including arsenite treatment and heat shock (Colombrita et al., 2009; Liu-Yesucevitz et al., 2010; McDonald et al., 2011; Nishimoto et al., 2010). Although TDP-43 was seen as a component of SGs under EA treatment, majority of cytoplasmic TDP-43 was independent of SGs and was diffusely distributed. These findings suggest that there is SG-independent mechanism for cytoplasmic distribution of TDP-43 under oxidative stress induced by glutathione depletion.

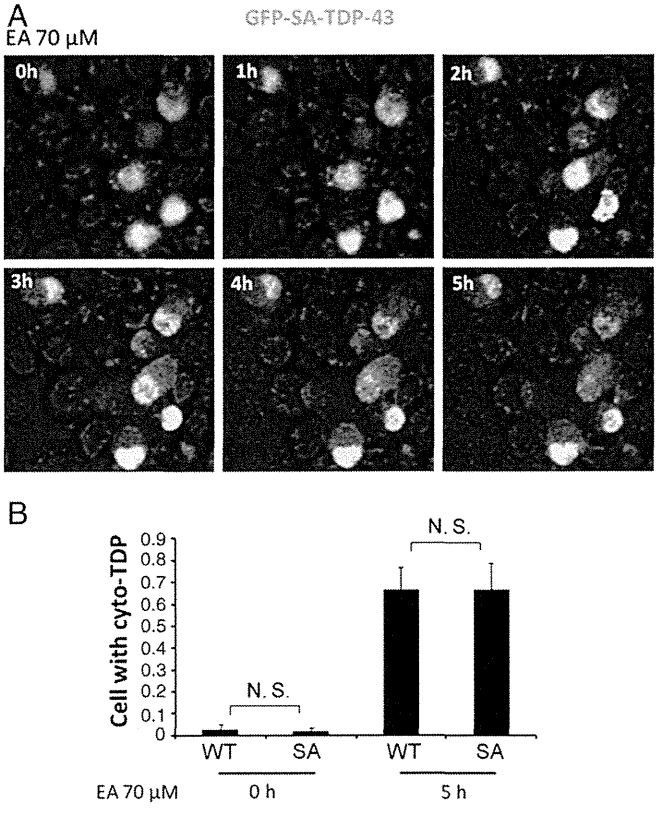

Fig. 6. The effect of C-terminal phosphorylation on TDP-43 distribution. (A) Time lapse analysis of NSC34 cells expressing GFP-SA-TDP-43. GFP-SA-TDP-43 was distributed to the cytoplasm by 70 μM of EA. (B) The proportion of cells with cytoplasmic distribution of TDP-43 (cells with cyto-TDP) in the GFP-TDP-43 expressing cells. The proportion of cells with cyto-TDP was not different between WT- and SA-TDP-43, either 0 h or 5 h after EA induction. Three areas per sample were measured. Error bars indicate SD.

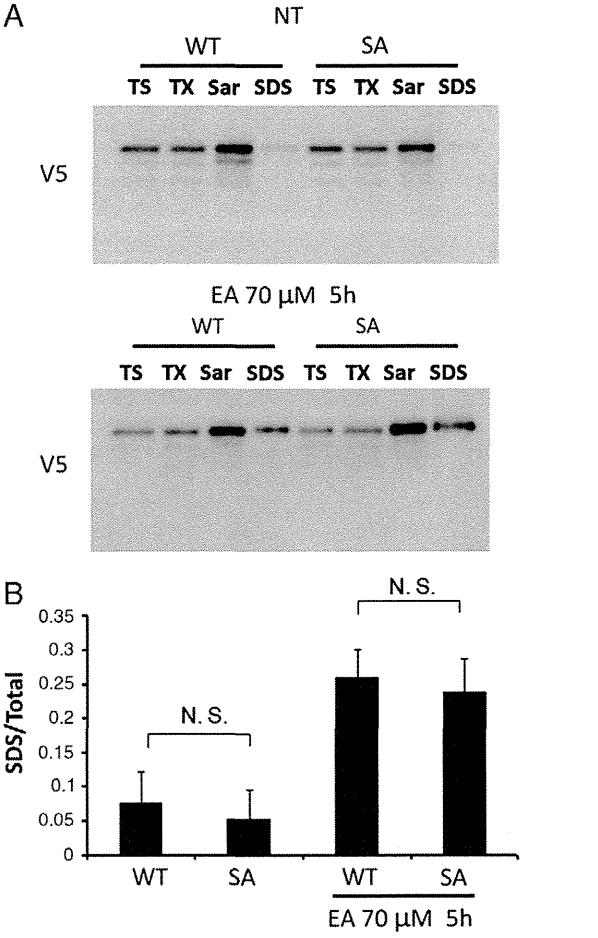

Fig. 7. The effect of C-terminal phosphorylation on TDP-43 solubility. (A) Sequential extraction of NSC34 cells expressing V5-WT- or V5-SA-TDP-43. (B) Densitometric quantitation of Sar-insoluble V5-TDP-43. Ratio of Sar-insoluble fraction from the whole fraction did not differ between WT- and SA-TDP-43 with or without 70 μM EA. Three independent experiments were performed. Error bars indicate SD.

In the present study, S403/404 and S409/410 of TDP-43 were phosphorylated together with insolubilization and cytoplasimic distribution of the protein. The hyperphosphorylation of disease marker proteins is a common feature of neurodegenerative disorders, and its relation to the pathogenesis has been intensively investigated: Tau in AD; huntingtin in HD; and alfa-synuclein in PD and DLB (Ballatore et al., 2007; Fujiwara et al., 2002; Gu et al., 2009). A number of studies have demonstrated that disease-specific phosphorylation of these marker proteins modulates aggregation and potentially influences disease pathogenesis (Azeredo da Silveira et al., 2009; Gu et al., 2009). In the present study, there was no difference between wild type and non-phosphorylable TDP-43 in the degree of insolubilization and cytoplasmic translocation under oxidative stress conditions, suggesting that C-terminal phosphorylation of TDP-43 is not mandatory for aggregation or abnormal intracellular distribution. In support with our findings, there is a study demonstrating that C-terminal phosphorylation of TDP-43 is not substantially required for the cytoplasmic aggregation (Brady et al., 2010). In addition, our results show that C-terminal tags interfere with the detection of TDP-43 phosphorylation, providing a cautionary note for cell-based and animal studies of TDP-43 with a C-terminal tag.

We further examined whether the pathological modifications of TDP-43 contribute to cell vulnerability to glutathione depletion. In the analysis of MTS assay, the viabilities of NSC34 cells were decreased by EA treatment. Although GFP-WT-TDP-43 was fully phosphorylated, insolubilized and distributed to cytoplasm in the cells treated with EA, there was no significant difference in the viability between the cells expressing GFP-mock and GFP-WT-TDP-43. In addition, the viability of NSC34 cells expressing GFP-SA-TDP-43 was not different from that of the cells expressing GFP-WT-TDP-43. These findings suggest that TDP-43 modification may not affect cell viability under oxidative stress induced by glutathione depletion.

In conclusion, we demonstrated that oxidative stress induced by glutathione depletion instigated TDP-43 modifications including C-terminal phosphorylation, insolubilization, C-terminal fragmentation and cytoplasmic distribution, and that these changes reproduce the pathological features of TDP-43 proteinopathies and other neurodegenerative diseases such as AD.

Supplementary materials related to this article can be found online at doi:10.1016/j.nbd.2011.12.002.

Funding

Funding: This work was supported by a Center-of-Excellence (COE) grant, a Grant-in-Aid for Scientific Research on Innovated Areas "Foundation of Synapse and Neurocircuit Pathology," and Grant-in-Aids from Ministry of Education, Culture, Sports, Science, and Technology of Japan; grants from the Ministry of Health, Labor and Welfare of Japan; and Core Research for Evolutional Science and Technology (CREST) of the Japan Science and Technology Agency (JST).

References

Abe, K., et al., 1995. Induction of nitrotyrosine-like immunoreactivity in the lower motor neuron of amyotrophic lateral sclerosis. Neurosci. Lett. 199, 152–154.

Abe, K., et al., 1997. Upregulation of protein-tyrosine nitration in the anterior horn cells of amyotrophic lateral sclerosis. Neurol. Res. 19, 124–128.
Amador-Ortiz, C., et al., 2007. TDP-43 immunoreactivity in hippocampal sclerosis and Alzheimer's disease. Ann. Neurol. 61, 435–445.
Arai, T., et al., 2006. TDP-43 is a component of ubiquitin-positive tau-negative inclusions in frontotemporal lobar degeneration and amyotrophic lateral sclerosis. Biochem. Biophys. Res. Commun. 351, 602–611.
Arai, T., et al., 2009. Phosphorylated TDP-43 in Alzheimer's disease and dementia with Lewy bodies. Acta Neuropathol. 117, 125–136.
Arai, T., et al., 2010. Phosphorylated and cleaved TDP-43 in ALS, FTLD and other neurodegenerative disorders and in cellular models of TDP-43 proteinopathy. Neuropathology 30, 170–181.
Ayala, Y.M., et al., 2005. Human, Drosophila, and C.elegans TDP43: nucleic acid binding properties and splicing regulatory function. J. Mol. Biol. 348, 575–588.
Ayala, Y.M., et al., 2008. TDP-43 regulates retinoblastoma protein phosphorylation through the repression of cyclin-dependent kinase 6 expression. Proc. Natl. Acad. Sci. U. S. A. 105, 3785–3789.
Azeredo da Silveira, S., et al., 2009. Phosphorylation does not prompt, nor prevent, the formation of alpha-synuclein toxic species in a rat model of Parkinson's disease. Hum. Mol. Genet. 18, 872–887.
Ballatore, C., et al., 2007. Tau-mediated neurodegeneration in Alzheimer's disease and related disorders. Nat. Rev. Neurosci. 8, 663–672.
Beal, M.F., et al., 1997. Increased 3-nitrotyrosine in both sporadic and familial amyotrophic lateral sclerosis. Ann. Neurol. 42, 644–654.
Brady, O.A., et al., 2010. Regulation of TDP-43 aggregation by phosphorylation and p62/SQSTM1. J. Neurochem. 116, 248–259.
Buratti, E., et al., 2005. TDP-43 binds heterogeneous nuclear ribonucleoprotein A/B through its C-terminal tail: an important region for the inhibition of cystic fibrosis transmembrane conductance regulator exon 9 splicing. J. Biol. Chem. 280, 37572–37584.
Buratti, E., et al., 2010. Nuclear factor TDP-43 can affect selected microRNA levels. FEBS J. 277, 2268–2281.
Butterfield, D.A., et al., 2007. Roles of amyloid beta-peptide-associated oxidative stress and brain protein modifications in the pathogenesis of Alzheimer's disease and mild cognitive impairment. Free Radic. Biol. Med. 43, 658–677.
Caragounis, A., et al., 2010. Zinc induces depletion and aggregation of endogenous TDP-43. Free Radic. Biol. Med. 48, 1152–1161.
Colombrita, C., et al., 2009. TDP-43 is recruited to stress granules in conditions of oxidative insult. J. Neurochem. 111, 1051–1061.
Dormann, D., et al., 2009. Proteolytic processing of TAR DNA binding protein-43 by caspases produces C-terminal fragments with disease defining properties independent of progranulin. J. Neurochem. 110, 1082–1094.
Ferrante, R.J., et al., 1997. Evidence of increased oxidative damage in both sporadic and familial amyotrophic lateral sclerosis. J. Neurochem. 69, 2064–2074.
Frederickson, C.J., et al., 2005. The neurobiology of zinc in health and disease. Nat. Rev. Neurosci. 6, 449–462.
Fujiwara, H., et al., 2002. alpha-Synuclein is phosphorylated in synucleinopathy lesions. Nat. Cell Biol. 4, 160–164.
Geser, F., et al., 2008. Pathological TDP-43 in parkinsonism-dementia complex and amyotrophic lateral sclerosis of Guam. Acta Neuropathol. 115, 133–145.
Gu, X., et al., 2009. Serines 13 and 16 are critical determinants of full-length human mutant huntingtin induced disease pathogenesis in HD mice. Neuron 64, 828–840.
Hasegawa, M., et al., 2007. TDP-43 is deposited in the Guam parkinsonism-dementia complex brains. Brain 130, 1386–1394.
Hasegawa, M., et al., 2008. Phosphorylated TDP-43 in frontotemporal lobar degeneration and amyotrophic lateral sclerosis. Ann. Neurol. 64, 60–70.
Igaz, L.M., et al., 2009. Expression of TDP-43 C-terminal Fragments in Vitro Recapitulates Pathological Features of TDP-43 Proteinopathies. J. Biol. Chem. 284, 8516–8524.
Iguchi, Y., et al., 2009. TDP-43 depletion induces neuronal cell damage through dysregulation of Rho family GTPases. J. Biol. Chem. 284, 22059–22066.
Keelan, J., et al., 2001. Quantitative imaging of glutathione in hippocampal neurons and glia in culture using monochlorobimane. J. Neurosci. Res. 66, 873–884.
Liu-Yesucevitz, L., et al., 2010. Tar DNA binding protein-43 (TDP-43) associates with stress granules: analysis of cultured cells and pathological brain tissue. PLoS One 5, e13250.
Lovell, M.A., Markesbery, W.R., 2007. Oxidative DNA damage in mild cognitive impairment and late-stage Alzheimer's disease. Nucleic Acids Res. 35, 7497–7504.
McDonald, K.K., et al., 2011. TAR DNA-binding protein 43 (TDP-43) regulates stress granule dynamics via differential regulation of G3BP and TIA-1. Hum. Mol. Genet. 20, 1400–1410.
Migliore, L., 2005. Searching for the role and the most suitable biomarkers of oxidative stress in Alzheimer's disease and in other neurodegenerative diseases. Neurobiol. Aging 26, 587–595.
Moisse, K., et al., 2009. Divergent patterns of cytosolic TDP-43 and neuronal progranulin expression following axotomy: implications for TDP-43 in the physiological response to neuronal injury. Brain Res. 1249, 202–211.
Neumann, M., et al., 2006. Ubiquitinated TDP-43 in frontotemporal lobar degeneration and amyotrophic lateral sclerosis. Science 314, 130–133.
Nishimoto, Y., et al., 2010. Characterization of alternative isoforms and inclusion body of the TAR DNA-binding protein-43. J. Biol. Chem. 285, 608–619.
Nonaka, T., et al., 2009a. Phosphorylated and ubiquitinated TDP-43 pathological inclusions in ALS and FTLD-U are recapitulated in SH-SY5Y cells. FEBS Lett. 583, 394–400.
Nonaka, T., et al., 2009b. Truncation and pathogenic mutations facilitate the formation of intracellular aggregates of TDP-43. Hum. Mol. Genet. 18, 3353–3364.
Nunomura, A., et al., 2002. Neuronal RNA oxidation is a prominent feature of dementia with Lewy bodies. Neuroreport 13, 2035–2039.
Polymenidou, M., et al., 2011. Long pre-mRNA depletion and RNA missplicing contribute to neuronal vulnerability from loss of TDP-43. Nat. Neurosci. 14, 459–468.
Rizzardini, M., et al., 2003. Mitochondrial dysfunction and death in motor neurons exposed to the glutathione-depleting agent ethacrynic acid. J. Neurol. Sci. 207, 51–58.
Sato, T., et al., 2009. Axonal ligation induces transient redistribution of TDP-43 in brainstem motor neurons. Neuroscience 164, 1565–1578.
Sephton, C.F., et al., 2011. Identification of neuronal RNA targets of TDP-43-containing ribonucleoprotein complexes. J. Biol. Chem. 286, 1204–1215.
Shaw, I.C., et al., 1995. Studies on cellular free radical protection mechanisms in the anterior horn from patients with amyotrophic lateral sclerosis. Neurodegeneration 4, 391–396.
Strong, M.J., et al., 2007. TDP43 is a human low molecular weight neurofilament (hNFL) mRNA-binding protein. Mol. Cell. Neurosci. 35, 320–327.
Tollervey, J.R., et al., 2011. Characterizing the RNA targets and position-dependent splicing regulation by TDP-43. Nat. Neurosci. 14, 452–458.
Wang, I.F., et al., 2002. Higher order arrangement of the eukaryotic nuclear bodies. Proc. Natl. Acad. Sci. U. S. A. 99, 13583–13588.
Wang, H.Y., et al., 2004. Structural diversity and functional implications of the eukaryotic TDP gene family. Genomics 83, 130–139.
Winton, M.J., et al., 2008. Disturbance of nuclear and cytoplasmic TAR DNA-binding protein (TDP-43) induces disease-like redistribution, sequestration, and aggregate formation. J. Biol. Chem. 283, 13302–13309.
Zhang, Y.J., et al., 2007. Progranulin mediates caspase-dependent cleavage of TAR DNA binding protein-43. J. Neurosci. 27, 10530–10534.

Neurobiology of Disease 41 (2011) 111–118

Contents lists available at ScienceDirect

Neurobiology of Disease

journal homepage: www.elsevier.com/locate/ynbdi

Mitochondrial membrane potential decrease caused by loss of PINK1 is not due to proton leak, but to respiratory chain defects

Taku Amo [a,1], Shigeto Sato [b], Shinji Saiki [b], Alexander M. Wolf [a], Masaaki Toyomizu [c], Clement A. Gautier [d], Jie Shen [d], Shigeo Ohta [a], Nobutaka Hattori [b,*]

[a] Department of Biochemistry and Cell Biology, Institute of Development and Aging Sciences, Graduate School of Medicine, Nippon Medical School, 1-396 Kosugi-cho, Nakahara-ku, Kawasaki 211-8533, Japan
[b] Department of Neurology, Juntendo University School of Medicine, 2-1-1 Hongo, Bunkyo-ku, Tokyo 113-8421, Japan
[c] Animal Nutrition, Life Sciences, Graduate School of Agricultural Science, Tohoku University, 1-1 Tsutsumidori-Amamiyamachi, Aoba-ku, Sendai 981-8555, Japan
[d] Center for Neurologic Diseases, Brigham and Women's Hospital, Program in Neuroscience, Harvard Medical School, Boston, MA 02115, USA

ARTICLE INFO

Article history:
Received 29 June 2010
Revised 17 August 2010
Accepted 25 August 2010
Available online 15 September 2010

Keywords:
Parkinson's disease
Mitochondria
PINK1
Parkin
Membrane potential
Oxidative phosphorylation
Modular kinetic analysis
Proton leak
Reactive oxygen species

ABSTRACT

Mutations in *PTEN-induced putative kinase 1* (*PINK1*) cause a recessive form of Parkinson's disease (PD). PINK1 is associated with mitochondrial quality control and its partial knock-down induces mitochondrial dysfunction including decreased membrane potential and increased vulnerability against mitochondrial toxins, but the exact function of PINK1 in mitochondria has not been investigated using cells with null expression of PINK1. Here, we show that loss of PINK1 caused mitochondrial dysfunction. In PINK1-deficient ($PINK1^{-/-}$) mouse embryonic fibroblasts (MEFs), mitochondrial membrane potential and cellular ATP levels were decreased compared with those in littermate wild-type MEFs. However, mitochondrial proton leak, which reduces membrane potential in the absence of ATP synthesis, was not altered by loss of PINK1. Instead, activity of the respiratory chain, which produces the membrane potential by oxidizing substrates using oxygen, declined. H_2O_2 production rate by $PINK1^{-/-}$ mitochondria was lower than $PINK1^{+/+}$ mitochondria as a consequence of decreased oxygen consumption rate, while the proportion (H_2O_2 production rate per oxygen consumption rate) was higher. These results suggest that mitochondrial dysfunctions in PD pathogenesis are caused not by proton leak, but by respiratory chain defects.

Introduction

Parkinson's disease (PD) is a neurodegenerative disease characterized by loss of dopaminergic neurons in the substantia nigra. Mitochondrial dysfunction has been proposed as a major factor in the pathogenesis of sporadic and familial PD (Abou-Sleiman et al., 2006). In particular, the identification of mutations in *PTEN-induced putative kinase 1* (*PINK1*) has strongly implicated mitochondrial dysfunction owing to its loss of function in the pathogenesis of PD (Valente et al., 2004). PINK1 contains an N-terminal mitochondrial targeting sequence (MTS) and a serine/threonine kinase domain (Valente et al., 2004). PINK1 kinase activity is crucial for mitochondrial maintenance via TRAP phosphorylation (Pridgeon et al., 2007). Loss of PINK1 function induces increased vulnerability to various stresses (Exner et al., 2007; Haque et al., 2008; Pridgeon et al., 2007; Wood-Kaczmar et al., 2008). However, silencing of PINK1 has only been partial and only one study has been performed to assess mitochondrial functions in steady and artificial states with complete ablation of PINK1 expression (Gautier et al., 2008).

Several studies have shown that PINK1 acts upstream of parkin in the same genetic pathway (Clark et al., 2006; Park et al., 2006) and co-overexpressed PINK1 and parkin both co-localized to mitochondria (Kim et al., 2008). Overexpression of PINK1 promotes mitochondrial fission (Yang et al., 2008). Fission followed by selective fusion segregates dysfunctional mitochondria and permits their removal by autophagy (Twig et al., 2008). PINK1 loss-of-function decreases mitochondrial membrane potential (Chu, 2010) and the PINK1–parkin pathway is associated with mitochondrial elimination in cultured cells treated with the mitochondrial uncoupler carbonyl cyanide *m*-chlorophenylhydrazone (CCCP), which causes mitochondrial depolarization (Geisler et al., 2010; Kawajiri et al., 2010; Matsuda et al., 2010; Narendra et al., 2008, 2010; Vives-Bauza et al., 2010). However, the exact mechanism underlying the mitochondrial depolarization induced by PINK1 defects leading to mitochondrial autophagy has not been examined in detail.

Abbreviations: $\Delta\psi$, mitochondrial membrane potential; FCCP, carbonyl cyanide p-trifluoromethoxyphenylhydrazone; MEFs, mouse embryonic fibroblasts; PD, Parkinson's disease; PINK1, PTEN-induced putative kinase 1; ROS, reactive oxygen species; TMRM, tetramethylrhodamine methyl ester; TPMP, triphenylmethylphosphonium.

* Corresponding author. Fax: +81 3 5800 0547.
E-mail address: nhattori@juntendo.ac.jp (N. Hattori).
[1] Present address: Department of Applied Chemistry, National Defense Academy, 1-10-20 Hashirimizu, Yokosuka 239-8686, Japan.

Available online on ScienceDirect (www.sciencedirect.com).

0969-9961/$ – see front matter © 2010 Elsevier Inc. All rights reserved.
doi:10.1016/j.nbd.2010.08.027

Here, we describe a detailed characterization of mitochondria in PINK1-deficient cells. We show that PINK1 deficiency causes a decrease in mitochondrial membrane potential, which is not due to proton leak, but to respiratory chain defects.

Materials and methods

PINK1 knock-out mouse embryonic fibroblasts (MEFs)

PINK1 knock-out MEFs were prepared and cultured as described previously (Matsuda et al., 2010). Mouse embryonic fibroblasts (MEFs) were derived from E12.5 embryos containing littermate 4 mice of each genotype. Embryos were mechanically dispersed by repeated passage through a P1000 pipette tip and plated with MEF media containing DME, 10% FCS, 1× nonessential amino acids, 1 mM L-glutamine, penicillin/streptomycin (invitrogen). The ψ2 cell line, an ecotropic retrovirus packaging cell line, was maintained in Dulbecco's modified Eagle medium (DMEM, Sigma) with 5% fetal bovine serum and 50 μg/ml kanamicin. Transfection of the ψ2 cells with pMESVTS plasmids containing an SV40 large T antigen was performed by lipofection method according to the manual provided by the manufacturer (GIBCO BRL). Five micrograms of the plasmids was used for each transfection. Transfectants were selected by G418 at the concentration of 0.5 mg/ml, and 10 clonal cell lines were established. The highest titer of 5×10^4 cfu/ml was obtained for the conditioned medium of a cell line designated ψ2SVTS1. 10^6 MEFs were plated onto a 10-cm culture dish and kept at 33 °C for 48 hours. Then medium was replaced with 2 ml supplemented with polybrene-supplemented medium conditioned by the ψ2SVTS1 cells at confluency for 3 days. Infection was continued for 3 hours, and the medium was replaced with a fresh one. The infected MEFs were cultured at 33 °C until immortalized cells were obtained.

We confirmed that the differences we detected in this study were due to the PINK1 deficiency, not to artificial effects by immortalization, by measuring cellular respiration rates of not immortalized MEFs from other littermates (Supplemental figure). The respiration rates of not immortalized MEFs were slightly slower than those of immortalized MEFs, but the differences between $PINK1^{+/+}$ and $^{-/-}$ MEFs were consistent (Fig. 2A).

Cell growth

Cells were seeded in 12-well plates at density of $3\sim6\times10^3$ cells/well and incubated in DMEM high glucose medium (4.5 g/l glucose and 1 mM sodium pyruvate) supplemented with 10% fetal bovine serum. After a day, the medium was replaced with DMEM glucose-free medium supplemented with 1 g/l galactose, 1 mM sodium pyruvate and 10% fetal bovine serum (DMEM galactose medium) at 37 °C in an incubator with a humidified atmosphere of 5% CO_2. Cells were trypsinized and live cells were assessed by trypan blue dye exclusion.

Mitochondrial morphological changes

Cells were seeded in 6-well plates at 2.0×10^5/well and incubated in DMEM high glucose medium (4.5 g/l glucose and 1 mM sodium pyruvate) supplemented with 10% fetal bovine serum and 1% penicillin/streptomycin. After a day, the medium was replaced with DMEM glucose-free medium supplemented with 1 g/l galactose, 1 mM sodium pyruvate and 10% fetal bovine serum (DMEM galactose medium) at 37 °C in an incubator with a humidified atmosphere of 5% CO_2. 24 hours later, cells were fixed and immunostained with anti-Tom20 antibody to visualize mitochondria according to a protocol as previously described (Kawajiri et al., 2010). All images were obtained using an Axioplan 2 imaging microscope (Carl Zeiss, Oberkochen, Germany).

Cellular ATP levels

Intracellular ATP levels were determined by a cellular ATP assay kit (TOYO B-Net, Tokyo, Japan) according to the manufacturer's instructions using a Lumat LB9507 luminometer (Berthold Technology, Bad Wildbad, Germany).

Membrane potential

Fluorescence images were recorded using a multi-dimensional imaging workstation (AS MDW, Leica Microsystems, Wetzlar, Germany) with a climate chamber maintained at 37 °C. Fluorescence was quantified with a CCD camera (CoolSnap HQ, Roper Scientific, Princeton, NJ) using a 20× objective. Cells were stained for 1 hour with a non-quenching concentration (20 nM) of tetramethylrhodamine methyl ester (TMRM) in a 96-well plate. The cell-permeable cationic dye TMRM accumulates in mitochondria according to the Nernst equation. Nuclei were stained with 250 nM Hoechst 34580. Mitochondrial TMRM fluorescence was integrated in a 40-μm diameter circular area around the nucleus, and the minimum fluorescence in this area was subtracted as background fluorescence.

Cell respiration

Cell respiration was measured at 37 °C using the Oxygen Meter Model 781 and the Mitocell MT200 closed respiratory chamber (Strathkelvin Instruments, North Lanarkshire, United Kingdom). Cells were cultured in DMEM with 4.5 g/l of glucose supplemented with 10% FBS. Cells were then trypsinized and resuspended in Leibovitz's L-15 medium (Invitrogen) at density of 8.0×10^6 cells/ml. The oxygen respiration rate was measured under each of the following three conditions: basal rate (no additions); State 4 (no ATP synthesis) [after addition of 1 μg/ml oligomycin (Sigma)], uncoupled [after addition of 3 μM FCCP (carbonyl cyanide *p*-trifluoromethoxyphenylhydrazone; Sigma)] using Strathkelvin 949 Oxygen System. After sequential measurements, the endogenous respiration rate was determined by adding 1 μM rotenone + 2 μM myxothiazol.

Mitochondrial respiration and membrane potential

Mitochondria were prepared from cultured MEFs as previously described (Amo and Brand, 2007). Mitochondrial oxygen consumption with 5 mM succinate as a respiratory substrate was measured at 37 °C using a Clark electrode (Rank Brothers, Cambridge, United Kingdom) calibrated with air-saturated respiration buffer comprising 0.115 M KCl, 10 mM KH_2PO_4, 3 mM HEPES (pH 7.2), 2 mM $MgCl_2$, 1 mM EGTA and 0.3% (w/v) defatted BSA, assumed to contain 406 nmol atomic oxygen/ml (Reynafarje et al., 1985). Mitochondrial membrane potential ($\Delta\psi$) was measured simultaneously with respiratory activity using an electrode sensitive to the lipophilic cation $TPMP^+$ (triphenylmethylphosphonium) (Brand, 1995). Mitochondria were incubated at 0.5 mg/ml in the presence of 80 ng/ml nigericin (to collapse the pH gradient so that the proton motive force was expressed exclusively as $\Delta\psi$) and 2 μM rotenone (to inhibit complex I). The $TPMP^+$-sensitive electrode was calibrated with sequential additions of $TPMP^+$ up to 2 μM, then 5 mM succinate was added to initiate respiration. Experiments were terminated with 2 μM FCCP, allowing correction for any small baseline drift. $\Delta\psi$ was calculated from the distribution of $TPMP^+$ across the mitochondrial inner membrane using a binding correction factor of 0.35 mg protein/μl. Respiratory rates with 4 mM pyruvate + 1 mM malate as a substrate in State 3 (with 0.25 mM ADP) and State 4 (with 1 μg/ml oligomycin) were determined using the Oxygen Meter Model 781 and the Mitocell MT200 closed respiratory chamber (Strathkelvin Instruments).